NATIONAL BUREAU OF STANDARDS REPORT

10 140

COMPRESSIVE STRENGTH
OF
SLENDER CONCRETE MASONRY WALLS

<NBS>

U.S. DEPARTMENT OF COMMERCE

NATIONAL BUREAU OF STANDARDS

NATIONAL BUREAU OF STANDARDS

The National Bureau of Standards [1] was established by an act of Congress March 3, 1901. Today, in addition to serving as the Nation's central measurement laboratory, the Bureau is a principal focal point in the Federal Government for assuring maximum application of the physical and engineering sciences to the advancement of technology in industry and commerce. To this end the Bureau conducts research and provides central national services in four broad program areas. These are: (1) basic measurements and standards, (2) materials measurements and standards, (3) technological measurements and standards, and (4) transfer of technology.

The Bureau comprises the Institute for Basic Standards, the Institute for Materials Research, the Institute for Applied Technology, the Center for Radiation Research, the Center for Computer Sciences and Technology, and the Office for Information Programs.

THE INSTITUTE FOR BASIC STANDARDS provides the central basis within the United States of a complete and consistent system of physical measurement; coordinates that system with measurement systems of other nations; and furnishes essential services leading to accurate and uniform physical measurements throughout the Nation's scientific community, industry, and commerce. The Institute consists of an Office of Measurement Services and the following technical divisions:

> Applied Mathematics—Electricity—Metrology—Mechanics—Heat—Atomic and Molecular Physics—Radio Physics [2]—Radio Engineering [2]—Time and Frequency [2]—Astrophysics [2]—Cryogenics. [2]

THE INSTITUTE FOR MATERIALS RESEARCH conducts materials research leading to improved methods of measurement standards, and data on the properties of well-characterized materials needed by industry, commerce, educational institutions, and Government; develops, produces, and distributes standard reference materials; relates the physical and chemical properties of materials to their behavior and their interaction with their environments; and provides advisory and research services to other Government agencies. The Institute consists of an Office of Standard Reference Materials and the following divisions:

> Analytical Chemistry—Polymers—Metallurgy—Inorganic Materials—Physical Chemistry.

THE INSTITUTE FOR APPLIED TECHNOLOGY provides technical services to promote the use of available technology and to facilitate technological innovation in industry and Government; cooperates with public and private organizations in the development of technological standards, and test methodologies; and provides advisory and research services for Federal, state, and local government agencies. The Institute consists of the following technical divisions and offices:

> Engineering Standards—Weights and Measures — Invention and Innovation — Vehicle Systems Research—Product Evaluation—Building Research—Instrument Shops—Measurement Engineering—Electronic Technology—Technical Analysis.

THE CENTER FOR RADIATION RESEARCH engages in research, measurement, and application of radiation to the solution of Bureau mission problems and the problems of other agencies and institutions. The Center consists of the following divisions:

> Reactor Radiation—Linac Radiation—Nuclear Radiation—Applied Radiation.

THE CENTER FOR COMPUTER SCIENCES AND TECHNOLOGY conducts research and provides technical services designed to aid Government agencies in the selection, acquisition, and effective use of automatic data processing equipment; and serves as the principal focus for the development of Federal standards for automatic data processing equipment, techniques, and computer languages. The Center consists of the following offices and divisions:

> Information Processing Standards—Computer Information — Computer Services — Systems Development—Information Processing Technology.

THE OFFICE FOR INFORMATION PROGRAMS promotes optimum dissemination and accessibility of scientific information generated within NBS and other agencies of the Federal government; promotes the development of the National Standard Reference Data System and a system of information analysis centers dealing with the broader aspects of the National Measurement System, and provides appropriate services to ensure that the NBS staff has optimum accessibility to the scientific information of the world. The Office consists of the following organizational units:

> Office of Standard Reference Data—Clearinghouse for Federal Scientific and Technical Information [3]—Office of Technical Information and Publications—Library—Office of Public Information—Office of International Relations.

---

[1] Headquarters and Laboratories at Gaithersburg, Maryland, unless otherwise noted: mailing address Washington, D.C. 20234.
[2] Located at Boulder, Colorado 80302.
[3] Located at 5285 Port Royal Road, Springfield, Virginia 22151.

NATIONAL BUREAU OF STANDARDS REPORT

COMPRESSIVE STRENGTH
OF
SLENDER CONCRETE MASONRY WALLS

By

Felix Y. Yokel, Robert G. Mathey
and Robert D. Dikkers

<NBS>

U.S. DEPARTMENT OF COMMERCE
NATIONAL BUREAU OF STANDARDS

The contents of this report are not be used for advertising or promotional purposes. Citation of proprietary products does not constitute an official endorsement or approval by the National Bureau of Standards for use of such commercial products.

TABLE OF CONTENTS

SI CONVERSION UNITS

In view of present accepted practice in this country in this technological area, common U.S. units of measurement have been used throughout this paper. In recognition of the position of the USA as a signatory to the General Conference on Weights and Measures, which gave official status to the metric SI systems of units in 1960, we assist readers interested in making use of the coherent system of SI units, by giving conversion factors applicable to U.S. units used in this paper.

Length   1 in = 0.0254* meter
             1 ft = 0.3048* meter

Area   1 in^2 = 6.4516* x 10^{-4} $meter^2$
            1 ft^2 = 0.09290 $meter^2$

Force   1 lb(lbf) = 4.448 newton
            1 kip = 4448 newton

Pressure, Stress

          1 psi = 6895, $newton/meter^2$
          1 ksi = 6.895 x 10^6 $newton/meter^2$

Mass Volume

          1 lb/ft^3 (lbm/ft^3) = 16.02 $kilogram/meter^3$

Moment

          1 kip-in = 113.0 newton-meter

---

*Exactly

Compressive Strength of Slender

Concrete Masonry Walls*

By

Felix Y. Yokel, Robert G. Mathey

and Robert D. Dikkers

Sixty reinforced and unreinforced concrete masonry walls of
different slenderness ratios were tested to failure under
vertical loads applied axially and at various eccentricities.
Prism specimens, made of similar masonry units and mortars,
were also tested under the same loading conditions. Analysis
of test results indicates that wall strength can be
conservatively predicted by evaluating cross sectional wall
capacity on the basis of prism strength and reducing the
capacity for slenderness effects by evaluating the added
moments attributable to wall deflection. Test results were
also compared with allowable loads computed in accordance
with the current NCMA standard.

_____

1. INTRODUCTION AND OBJECTIVE

At the present time only a limited amount of experimental
data is available on the compressive strength of slender
concrete masonry walls. Present design practice accounts
for slenderness effects by stress correction factors [1]
or empirical equations [2]. The designer has no rational
method by which he can evaluate slenderness effects and
important parameters are not taken into consideration, such
as cross sectional properties, end support conditions, and
the relationship between compressive strength and elastic
properties of the masonry. With the increasing use of
load bearing masonry in the construction of multi-story
buildings, it is no longer adequate or economical to
disregard these parameters.

The objective of this investigation was to determine and
analyze the effect of wall slenderness and load eccentricity
on the strength of slender concrete masonry walls,
as a step in the development of rational design methods
for masonry walls subjected to axial and eccentric
vertical loads.

1

2.   SCOPE

Two wall systems were tested:

    1.   6-in reinforced concrete masonry walls.

    2.   8-in unreinforced concrete masonry walls.

For each of these wall systems specimens were constructed which were 4-ft wide and approximately 10, 16, and 20-ft high.[1/] These walls were tested to destruction under vertical loads which were applied axially and at eccentricities of 1/6, 1/4 and 1/3 of the wall thickness.

For each combination of wall height and load eccentricity, two companion specimens were tested. One of these specimens was instrumented to measure horizontal deflections and wall shortening under vertical loads. All of these specimens were tested at an approximate age of ten days. In addition, two 10-ft high and two 20-ft high walls of each wall system were tested axially at an age of more than 28 days to determine the strength increase with an additional curing period.

[1/] Hereafter in this report heights of walls are referred to as 10-ft, 16-ft and 20-ft. However, actual wall heights were 9 ft-3 5/8 in, 15 ft-11 5/8 in and 19 ft-3 5/8 in.

2

Following construction, four of the unreinforced walls
were found to have undersized block and increased joint
thicknesses as a consequence. These specimens were tested,
and an additional four specimens with correct joint size
were added to provide unbiased data. In all, 28 reinforced
walls and 32 unreinforced walls were tested.

An investigation of masonry prism strength under eccentric
compressive loads was also conducted by subjecting 8-in
and 6-in masonry prisms to the same loading conditions
that were used for the full scale walls. Two-block high
as well as three-block high prisms were tested in order
to determine the effect of prism height on the prism
strength. In addition, the comparative strength of prisms
with different thicknesses of mortar joints was investigated.

The investigation was completed by an analysis of results
which is presented in Section 6 of this report, and a
discussion of present design practice which is included
in Section 7.

3. TEST SPECIMENS

3.1. Materials

3.1.1. Masonry Units

Concrete masonry units used in the construction of test specimens were 8 x 8 x 16-in two-core hollow block, which were used in the unreinforced walls, and 6 x 8 x 16-in two-core hollow block which were used in the reinforced walls.

The units were made of a blend of light and normal weight aggregate (cinder and limestone). Cementitious material was portland cement and silica flour. The specified compressive strength of the units, based on net cross sectional area, was 3,000 psi. Actual average compressive strength of the units tested was 4230 psi and 4080 psi for the 8-in and the 6-in units respectively.

Dimensions and properties of the masonry units which were determined in accordance with ASTM standard C140-65T [3] are recorded in table 3.1. The masonry units used are illustrated in figure 3.1.
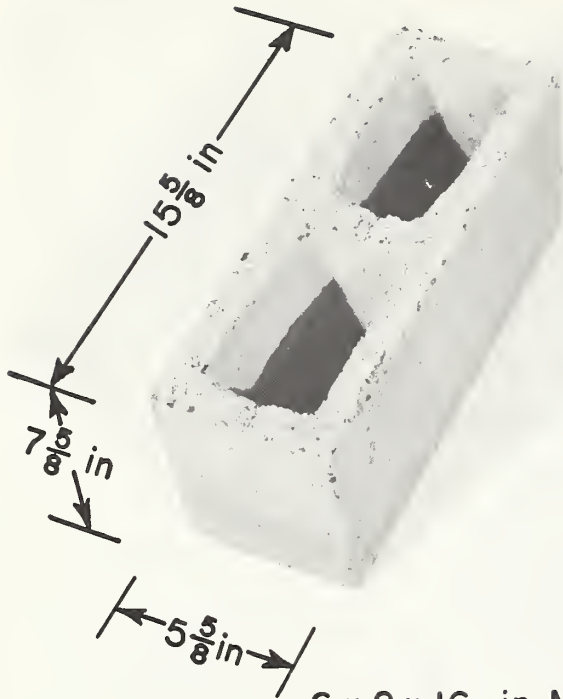
4

Table 3.1 Dimensions and Properties
of Concrete Masonry Units[a]

Unit	Width in	Height in	Length in	Minimum Thickness in. Face Shell	Web	Gross Area in²	Net Area %	Compressive Strength Gross Area psi	Net Area psi	Oven Dry Weight lb	Concrete Weight lb/ft³	Water Absorption lb/ft³
8-in block	7 5/8	7 5/8	15 19/32	1 5/16	1	118.90	52.33	2213	4230	29.71	108.20	11.32
6-in block	5 5/8	7 5/8	15 5/8	1	1	87.89	55.89	2280	4080	22.78	105.09	12.21

a/ Values given in the table represent the average results from tests
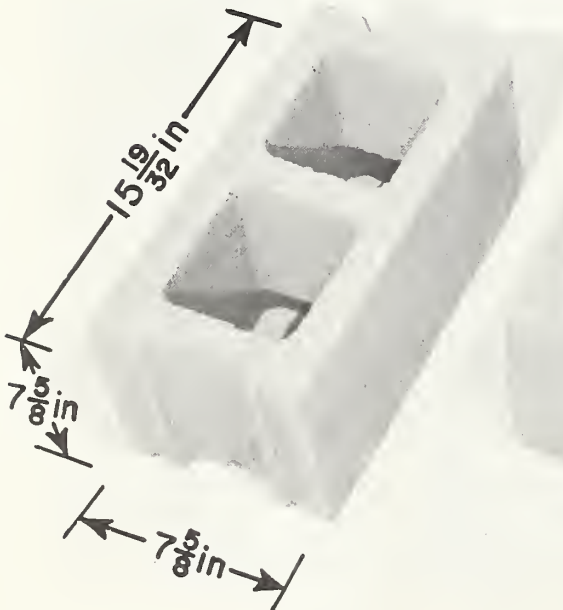or measurements of 5 units.

Corner Block   Lintel Block

6 x 8 x 16 - in Masonry Units

Stretcher
Block

Kerf
Block

Corner
Block

8 x 8 x 16 - in Masonry Units

MASONRY UNITS

Fig. 3.1

3.1.2. Mortar

Mortar used in the reinforced, as well as the unreinforced wall panels was type S mortar, in accordance with the proportion specifications of ASTM C 270 [4]. Type I portland cement, masonry cement and sand were proportioned 1/2:1:4 by volume. The sand was bank run siliceous aggregate from White Marsh, Maryland, with a fineness modulus of 1.73.

Forty-one sets of 2-in mortar cubes were made during the fabrication of the wall panels. The mortar cubes were made and stored under the same conditions as the wall panels. In general, the mortar cubes were tested at approximately the same age as the corresponding walls, however, some of the reinforced concrete masonry wall panels took 6 days to fabricate because of waiting time for two grouting operations and weekend delays. The age of tested mortar cubes, therefore, ranged from 9 to 53 days. Mortar cube strength averaged 1181 psi. Individual mortar cube tests are listed in table 3.2. As indicated in the table, the cube strengths ranged from 700 to 1768 psi. However 30 of the 41 sets of cubes had compressive strengths within 300 psi of the average value.

7

Table 3.2 Compressive Strength of Mortar Cubes

No. Test	Date of Fabrication	Date of Test	Age days	Average Compressive Strength psi
1	6/27/68	7/15/68	18	758
2	6/28/68	7/15/68	17	1166
3	7/1/68	7/15/68	14	1282
4	8/26/68	9/10/68	15	1271
5	7/3/68	7/23/68	20	950
6	7/5/68	7/23/68	18	1250
7	7/8/68	7/23/68	15	1006
8	7/9/68	7/23/68	14	1125
9	7/11/68	7/29/68	18	862
10	7/10/68	7/29/68	19	1768
11	7/12/68	7/29/68	17	1317
12	7/16/68	8/14/68	29	1139
13	7/16/68	8/14/68	29	1000
14	7/30/68	8/20/68	21	1309
15	7/31/68	8/20/68	20	1125
16	8/2/68	8/20/68	18	1500
17	8/6/68	8/20/68	14	1340
18	8/8/68	8/21/68	13	1175
19	7/9/68	7/18/68	9	1123
20	7/1/68	7/16/68	15	1244
21	7/2/68	7/16/68	14	1286
22	10/7/68	11/4/68	28	1628
23	10/7/68	10/14/68	7	967
24	9/20/68	10/2/68	12	1651
25	9/6/68	9/26/68	20	1438
26	9/10/68	9/26/68	16	915
27	9/13/68	9/27/68	14	1050
28	9/16/68	9/27/68	11	1414
29	9/17/68	9/27/68	10	1187
30	8/22/68	9/18/68	27	700
31	8/27/68	9/18/68	22	1267
32	8/29/68	9/18/68	20	736
33	9/3/68	9/18/68	15	1428
34	7/19/68	9/10/68	53	1208
35	7/22/68	9/10/68	50	1033
36	7/24/68	9/10/68	48	1149
37	7/26/68	9/10/68	46	1386
38	8/14/68	9/10/68	27	794
39	9/18/68	9/30/68	12	1354
40	9/18/68	9/30/68	12	1356
41	9/19/68	9/30/68	11	769

Average 1181

Since many batches of mortar were used in the construction of a wall panel and many of the walls took up to 6 days to fabricate, the mortar strength varied in different elevations of the wall.   However it is reasonable to assume that the average value of 1181 psi approximately represents ' the strength of the mortar in the wall panels.

3.1.3.   Grout

The grout used in the reinforced concrete masonry wall panels was a coarse grout in accordance with ASTM C 476 [5]. The grout mix had the following proportions by weight:

Type I Portland Cement	47 lb
Sand	120 lb
Gravel (3/8-in maximum size)	80 lb
Water	40 lb

Proportions of portland cement, sand and gravel by volume were 1:3:2.

The bank run sand and gravel were siliceous aggregates. The sand had a fineness modulus of 1.73. Gravel had a maximum size of 3/4-in.

Eleven 6 x 12-in grout cylinders were made during the fabrication of the reinforced masonry walls, and cured under similar conditions as the walls. The compressive strengths ranged from 1857 psi to 2900 psi and averaged 2290 psi when tested at ages from 8 to 47 days. Individual test results are tabulated in table 3.3. It was observed that in general the strengths increased with an increase in age of the grout cylinder. The cylinders tested at the least age, 8 days, gave the lowest compressive strength. Since the test results indicated that the majority of the cylinders, a total of 8, had compressive strengths within 300 psi of the average value, the average value of compressive strength can be assumed to be a representative value for all the grout cylinders.

It has been observed [6] that because of the water absorption by the masonry units, grout within the walls achieves a significantly higher strength than the same grout when cured as cylinders. It may therefore be assumed that the grout within the walls had a compressive strength higher than the 2290 psi cylinder strength.

3.1.4. Steel Reinforcement
Vertical and horizontal steel in the reinforced wall panels consisted of ASTM A615 [7] No. 5 deformed bars with a yield strength of 60,000 psi.

10

Table 3.3 Compressive Strength of Grout Cylinders

No. Test	Date of Fabrication	Date of Test	Age days	Wall Designation	Panel No.	Compressive Strength psi
1	7/24/68	9/9/68	47	20-R-0 20-R-0	1 2	2476
2	7/26/68	9/9/68	45	20-R-0 20-R-0	1 2	2264
3	7/10/68	7/23/68	13	16-R-T4 16-R-T4	5 6	1910
4	7/15/68	7/26/68	11	16-R-T4 16-R-T4	5 6	2009
5	8/2/68	8/17/68	15	16-R-T3 16-R-T3	7 8	2193
6	7/10/68	7/18/68	8	16-R-T6 16-R-T6	3 4	1857
7	From	9/27/68	28-39			2228
8	8/19	9/27/68	28-39			2900
9	to	9/27/68	28-39			2387
10	8/30	9/27/68	28-39			2546
11	9/6/68	9/27/68	21	20-R-T4 20-R-T4	7 8	2449

Average 2290

11

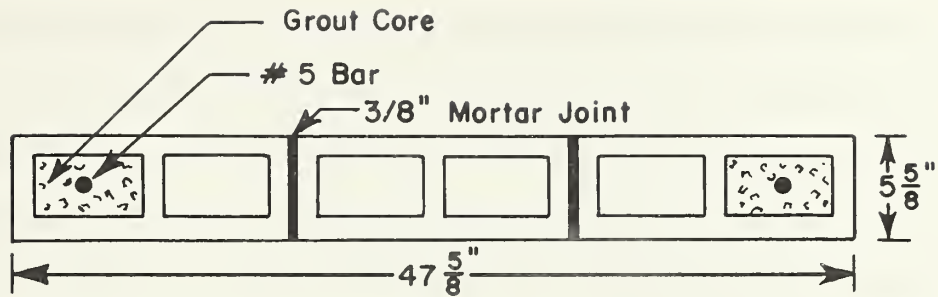## 3.2. Construction of Specimens

3.2.1. General

The wall panels and prisms were built and cured in the laboratory at approximately 73°F and 50% relative humidity. Wall panels were constructed in pairs between wooden guides to assure proper alignment and plumbness. Joint thickness was controlled at 3/8-in by horizontal lines at 16-in intervals which correspond to the height of two blocks and two joints. This method led to oversized joints in four unreinforced panels, where block which was undersized in height were used.
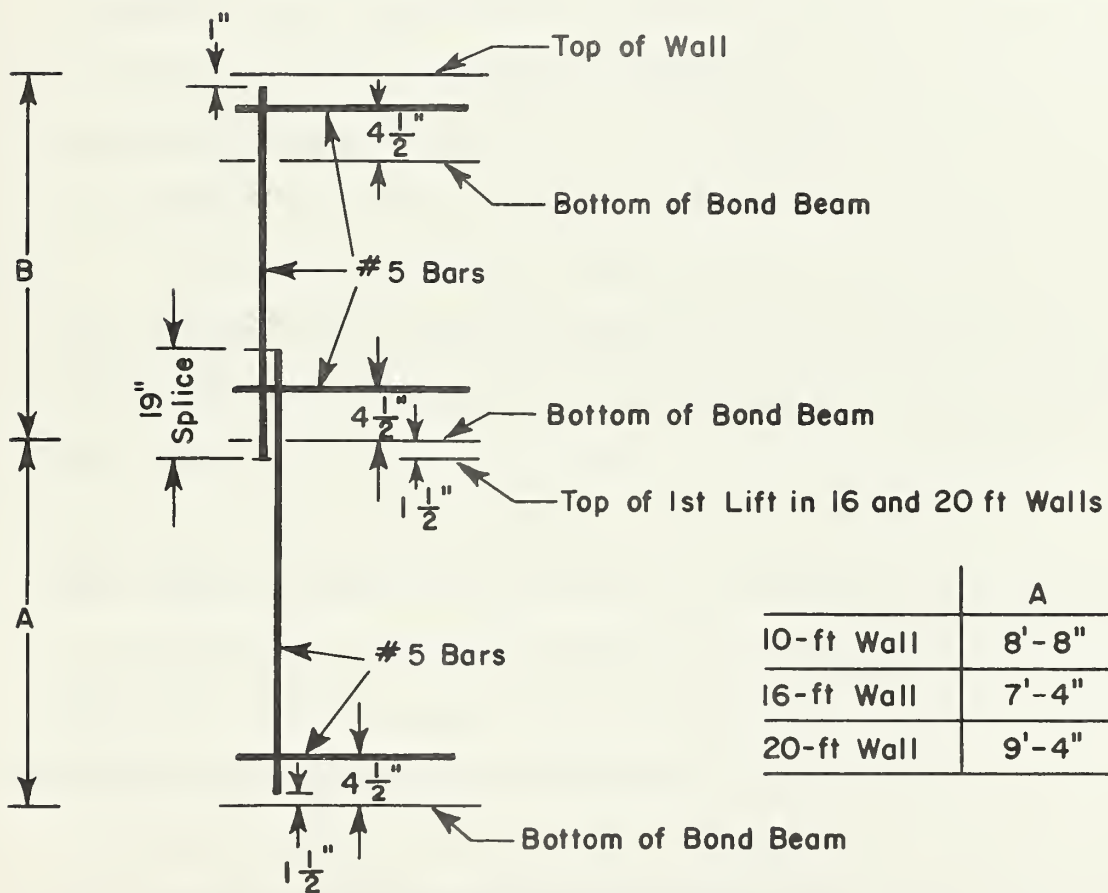
3.2.2. 6-in Reinforced Walls

Wall panels were constructed in three nominal sizes: 4 x 10-ft, 4 x 16-ft and 4 x 20-ft. Walls were built of the 6 x 8 x 16-in concrete block which were laid in running bond.

A wall cross section is shown in figure 3.2(a). Face shell bedding was used for the horizontal and vertical mortar joints, and mortar was also placed on the cross webs

12

Grout Core

#5 Bar

3/8" Mortar Joint

$5\frac{5}{8}"$

$47\frac{5}{8}"$

(a.) Typical Horizontal Section

1"

Top of Wall

$4\frac{1}{2}"$

Bottom of Bond Beam

B

#5 Bars

19" Splice

#5 Bars

$4\frac{1}{2}"$

Bottom of Bond Beam

$1\frac{1}{2}"$

Top of 1st Lift in 16 and 20 ft Walls

A

#5 Bars

$4\frac{1}{2}"$

$1\frac{1}{2}$

Bottom of Bond Beam

	A	B
10-ft Wall	8'- 8"	0'- $7\frac{5}{8}"$
16-ft Wall	7'- 4"	8'- $7\frac{5}{8}"$
20-ft Wall	9'- 4"	9'- $11\frac{5}{8}"$

(b) Reinforcement Details

6-IN REINFORCED WALLS

Fig. 3.2

around the cores which were to be grouted. Mortar joint
thickness was 3/8-in. One No. 5 bar was grouted into
each of the two outside cores of the wall as shown in
figure 3.2(a). Vertical bars in the 16-ft and the 20-
ft walls were spliced near nidheight over a length of
30 bar diameters (19-in). Horizontal reinforcement, consist-
ing of one No. 5 deformed bar was installed in each bond
beam as shown in figure 3.2(b). These bars were grouted
into 6 x 8 x 16-in lintel block laid horizontally. The
10-ft walls had bond beams at the top and bottom course,
whereas the 16 and 20-ft walls had an additional bond
beam at midheight. Actual cross sectional dimensions
of the walls were 47 5/8 in by 5 5/8 in; actual panel
heights were 9 ft - 3 5/8 in, 15 ft - 11 5/8 in, and 19
ft - 3 5/8 in.

Present design practice [2] specifies an area of steel not
less than 0.0013 times the cross sectional area of the
wall in one direction and not less than 0.0007 in the other
direction. The area of vertical steel used in the reinforced
walls of this investigation was equal to 0.0023 times the
cross sectional area, therefore, the area of principal
reinforcement was about twice the minimum area required.

14

The reinforced walls were constructed in the following
manner: The first course of each wall contained three
whole lintel units (see figure 3.1) which were laid on
a full mortar bed on a plastic sheet, placed on the
laboratory floor. These units formed a horizontal trough
into which the horizontal reinforcement could be grouted.
A strip of painted 2.5 lb/yd^2 diamond mesh metal lath
was placed over the top of these lintel units in the middle
32-in of the wall to contain the grout. Wall construction
was then continued to the bottom of the next bond beam
course.

After completion of every three courses of block, mortar
protrusions were removed from the two end cores by a 2-ft
long stick, to keep these cores clean for grouting.
Clean-out holes were provided at each end of the
bond beam. Sand was placed at the bottom of the vertical
cores to be grouted to facilitate removal of the mortar
droppings. Before grouting, the end cores and the bond
beam were inspected and cleaned by compressed air.

Horizontal and vertical reinforcement bars were then placed
and tied together, to prevent dislocation of the bars
during grouting. Prior to grouting, the clean-out holes
were covered by boards.

Walls were at least 16 hours old before grouting. In
the first few walls, grout was consolidated by rodding.
Subsequently, a vibrator was used to insure filling of
voids, particularly in the bond beams. Grout was poured
to within one inch from the top of the lift and reconsolidated
after 30 minutes to remove air voids caused by water absorp-
tion by the masonry units. The grout in the first lift
was permitted to set over night before construction of
the second half of the wall was started. The second half
of the 16-ft walls contained two bond beams which had
only two lintel blocks. At the outer end of these beams
regular half-block were used. Openings were cut into
these half-block to accommodate the horizontal bar and
to provide cleanout holes at mid height. In the 20-ft
walls all bond beams were built of three whole lintel
block. The upper bond beam of the 10-ft walls also consisted
of three whole lintel units. The 10-ft walls were constructed
in one lift. Two lifts were used in the 16 and 20-ft walls.

3.2.3. 8-in Unreinforced Walls

Wall panels, as in the case of the reinforced walls, were
constructed in nominal sizes of 4 x 10-ft, 4 x 16-ft and

16

4 x 20-ft. Walls were built in running bond with 8 x 8
x 16-in masonry units. Face shell bedding was used for
the horizontal and vertical joints and additional mortar
was placed on the cross webs at the two wall ends. Mortar
joint thickness was 3/8-in. Actual cross sectional dimen-
sions of the walls were 47 5/8 in x 7 5/8 in. Actual
wall heights were 9 ft - 3 5/8 in, 15 ft - 11 5/8 in and 19
ft - 3 5/8 in.

The first course was constructed from three whole masonry
units. Each alternate course contained two half-block
at the wall ends. Kerf block were used as half-block
and corner block were used where whole units were required
at the wall ends (refer to figure 3.1). A typical 20-ft
high wall panel is shown in figure 3.3.

3.2.4. Prism Specimens

Prism specimens were built in stacked bond using the
8 x 8 x 16-in block and the 6 x 8 x 16-in block. Mortar
was applied in face shell bedding as in the walls with
3/8-in thick mortar joints. Three-block high as well
as two-block high specimens were constructed.

Prisms were built at random during construction of the
walls, using the same mortar batches, and cured under

the same conditions as the walls. Before testing, prisms were capped with high strength plaster.
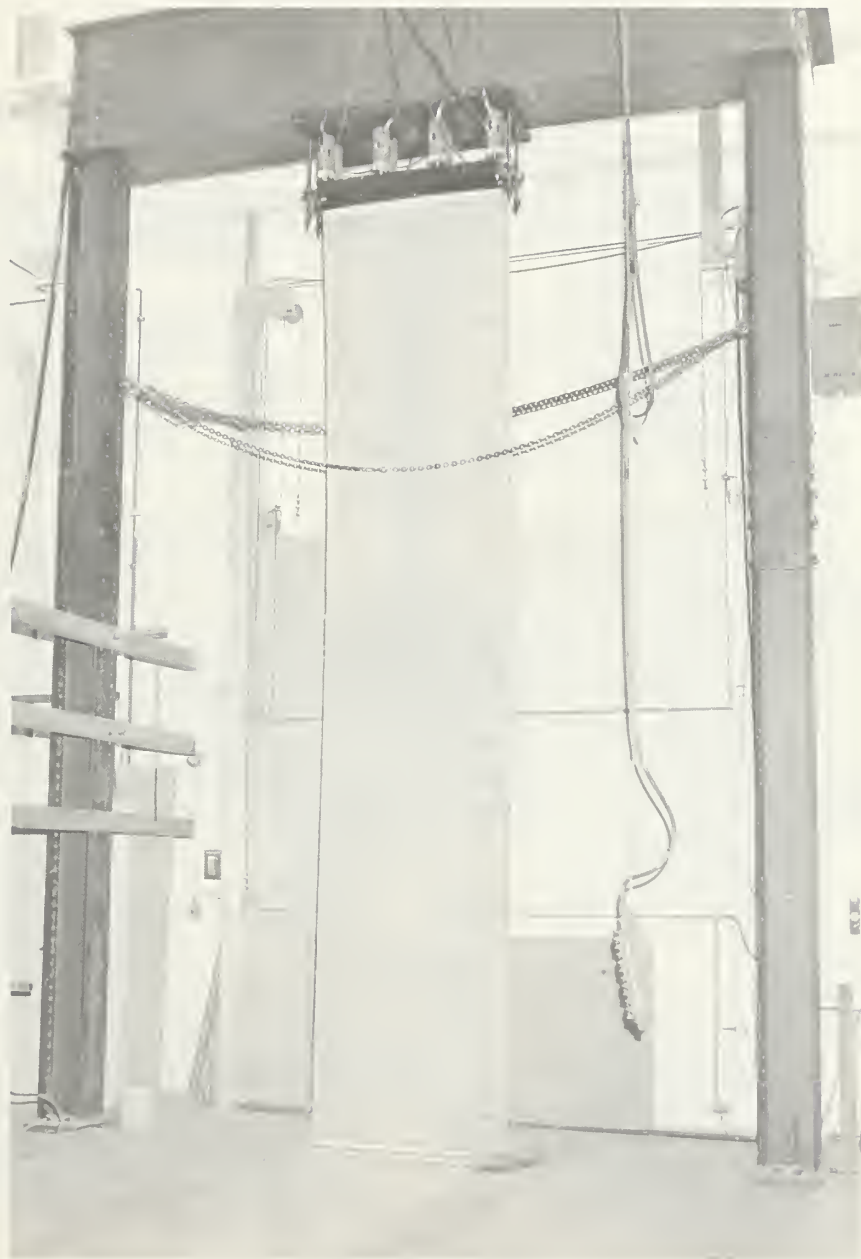
20-FT HIGH 8-IN UNREINFORCED
WALL PANEL

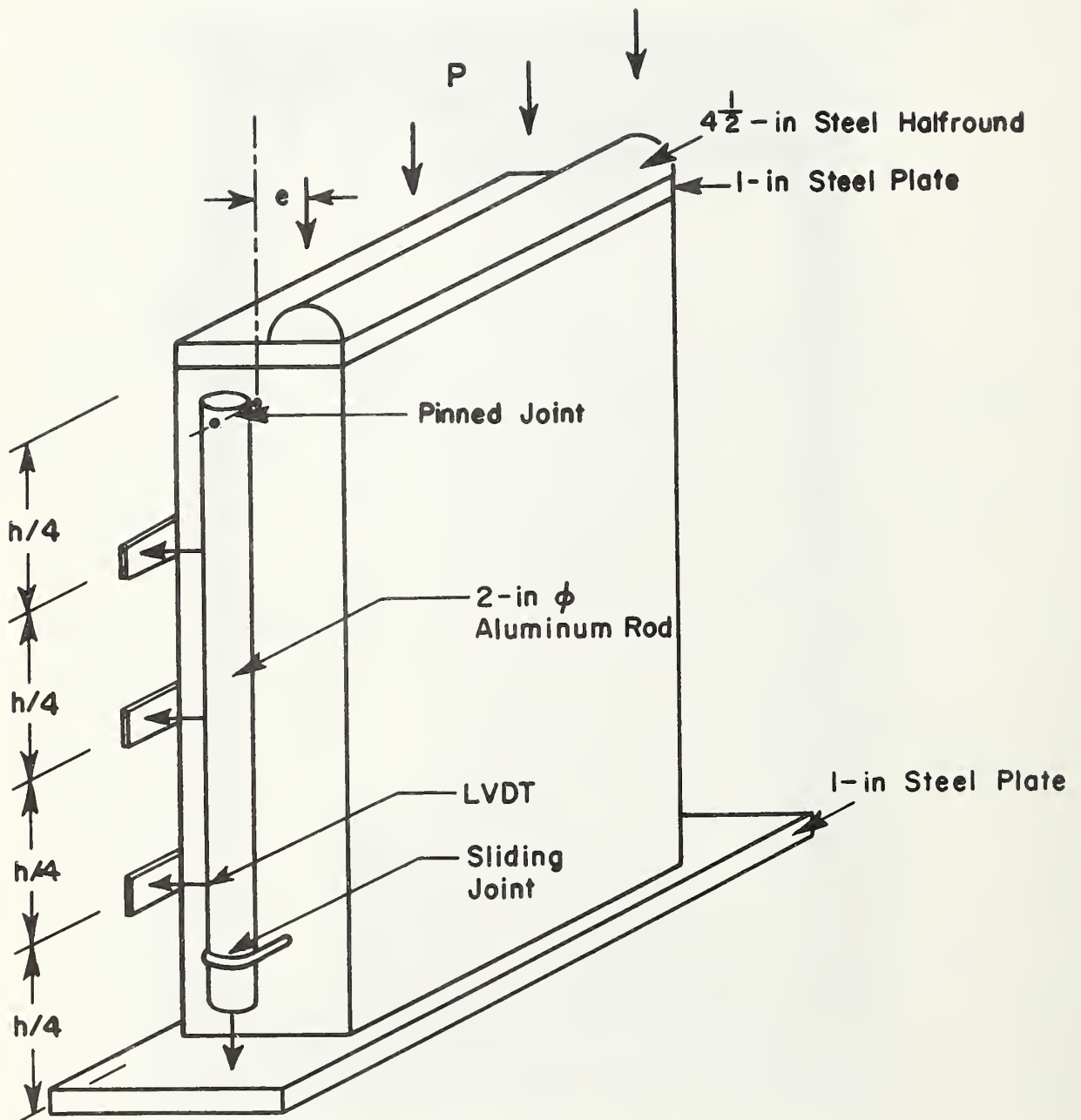Fig. 3.3

4. TEST PROCEDURE AND INSTRUMENTATION

Wall panels were tested in a steel frame with an adjustable top cross-beam that could be raised or lowered to accommodate the various wall heights. Eight 30-ton capacity hydraulic rams were attached to the cross-beam. Figure 4.1 shows the loading system and the frame with a 20-ft wall in place.

Figure 4.2 shows a diagram of the test set-up. At the base a 1-in thick steel plate was cemented to the laboratory floor by high strength plaster. The wall panel was set on top of this plate on another bed of high strength plaster. When the wall was set, care was taken to assure wall plumbness and alignment. Another 1-in thick steel plate was cemented to the top of the wall, to prevent wall failure by stress concentration. A 4 1/2-in diameter steel half-round was set on this steel plate with the flat side toward the wall. Load was applied to the curved top of this steel half-round through a 4-in thick steel plate which transmitted the load from the eight symmetrically-located hydraulic rams. The loading head is shown in figure 4.3. The test setup described above was designed to prevent rotation at the base of the wall, while permitting free
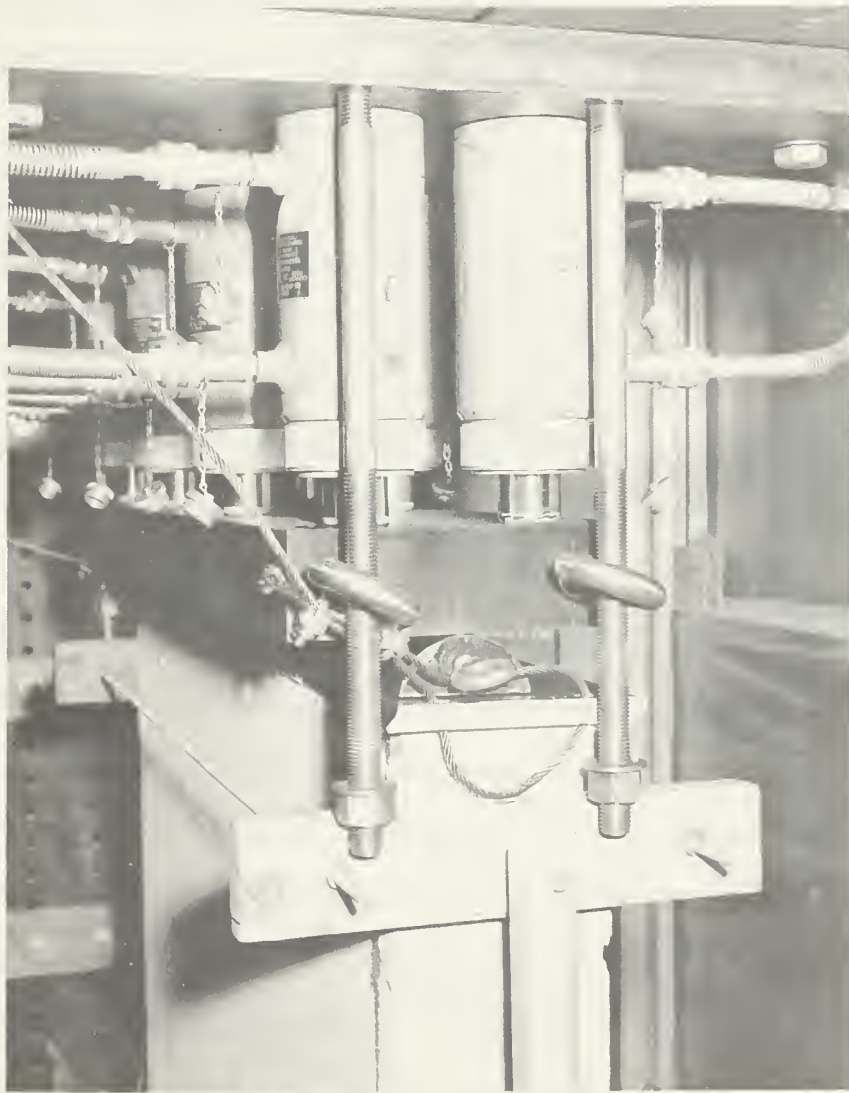
LOADING SYSTEM AND FRAME

Fig. 4.1

TEST SETUP

Fig. 4.2

LOADING HEAD

Fig. 4.3

rotation at the top. Great care was taken to position the wall and the steel half-round precisely in order to apply the load at the desired eccentricity. Wall instrumentation is also illustrated schematically in figure 4.2. Aluminum tubes of 2-in diameter were attached to the sides of the walls. At the upper end the tubes had a pinned connection to the wall and at the lower end they were attached to a guide which kept the tubes in line with the centerline of the wall but permitted them to slide downwards as the wall contracted under the load. For the first four 16-ft reinforced wall specimens, aluminum tubing of 1-in diameter was used. It was however observed that this tubing tended to deflect slightly, and 2-in diameter tubes were used in subsequent tests.

All instruments for the measurement of deflections were attached to these aluminum tubes. Horizontal deflections and wall shortenings were measured by linear variable differential transducers, capable of reading 0.0001 in. Instrument readings were electronically scanned at every 20 kip increment of vertical load and recorded in digital form. These data were manually key punched onto cards and automatically reduced, analyzed and plotted by electronic computer. Computer output consisted of tabulated test results and plotted load-deflection curves.
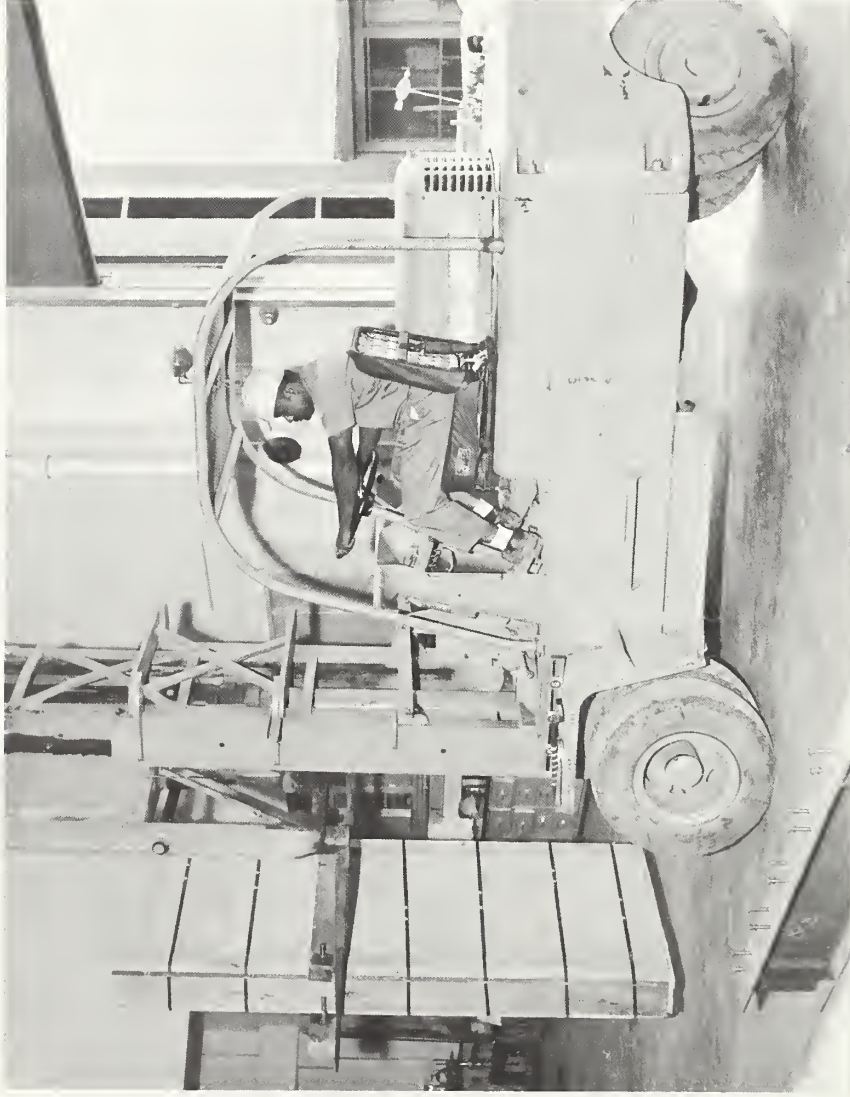
24

Instruments were installed to measure wall shortening and horizontal deflections at 1/4-height, mid-height and 3/4-height of the wall. Instruments were installed symmetrically at both wall ends.

One 10-ft unreinforced wall was also instrumented over a 24-in gage length on each wall face to determine the modulus of elasticity of the masonry.

Tests were carried out in duplicate for the same wall height and eccentricity. The first of the two walls tested was not instrumented and only failure load was recorded. The second specimen was instrumented, but instrumentation was removed at about 2/3 of the failure load of the first specimen. Deflection readings at wall failure are therefore not available. This procedure was adopted to protect instrumentation from damage by explosive wall failures.

Walls were moved from the fabrication area to the test frame by a fork lift truck. Before moving, the walls were carefully braced to prevent damage to the specimen. A wall being moved by the fork lift truck is shown in figure 4.4.

Prism specimens were tested in the same manner as the wall panels. The prisms were set in high strength plaster

WALL BEING MOVED TO THE TEST FRAME

Fig. 4.4

on a steel plate. A 1-in steel plate was set in plaster on top of the prisms, and load was applied by a 4 1/2-in steel half round. Three-block high, as well as two-block high prisms were tested in duplicate for each load eccentricity.

5.   TEST RESULTS

5.1.   6-in Reinforced Walls

Results of tests on the 6-in reinforced walls are presented
in table 5.1 and plotted in figure 5.1. Load-deflection
curves for these walls are shown in figures 5.2 through
5.4. The curves show deflections at 3/4 height of the
walls which are the maximum deflections.

Figure 5.5 shows typical wall failures. A log of all
recorded individual failures is presented in table 5.2.
The 10-ft high walls with small eccentricity of load failed
by vertical splitting and compression. The walls subjected
to the largest eccentricity of load failed by crushing
in the top 3 courses.

All of the 16-ft high walls failed along a horizontal
joint, approximately 1/4 the wall height from the top
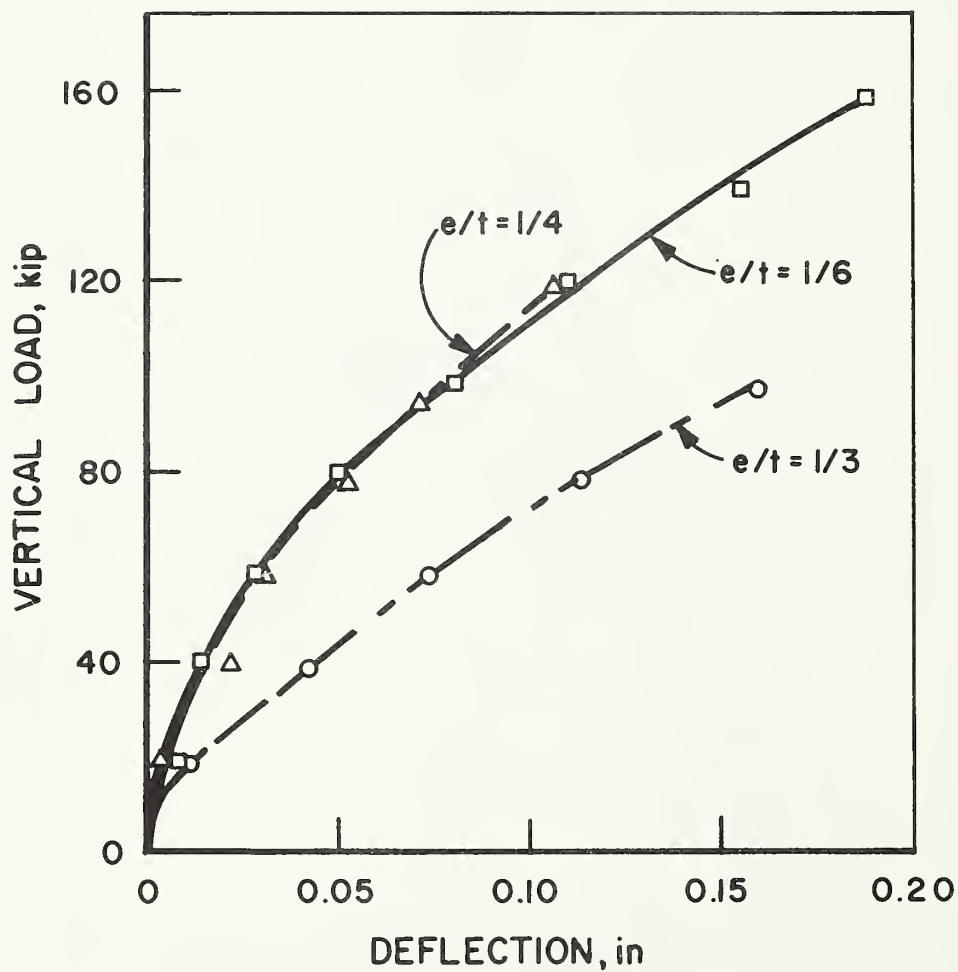of the wall. These walls developed large deflections
prior to failure.

The 20-ft high walls also failed at horizontal joints,
approximately 1/4 of the wall height from the top of the wall.
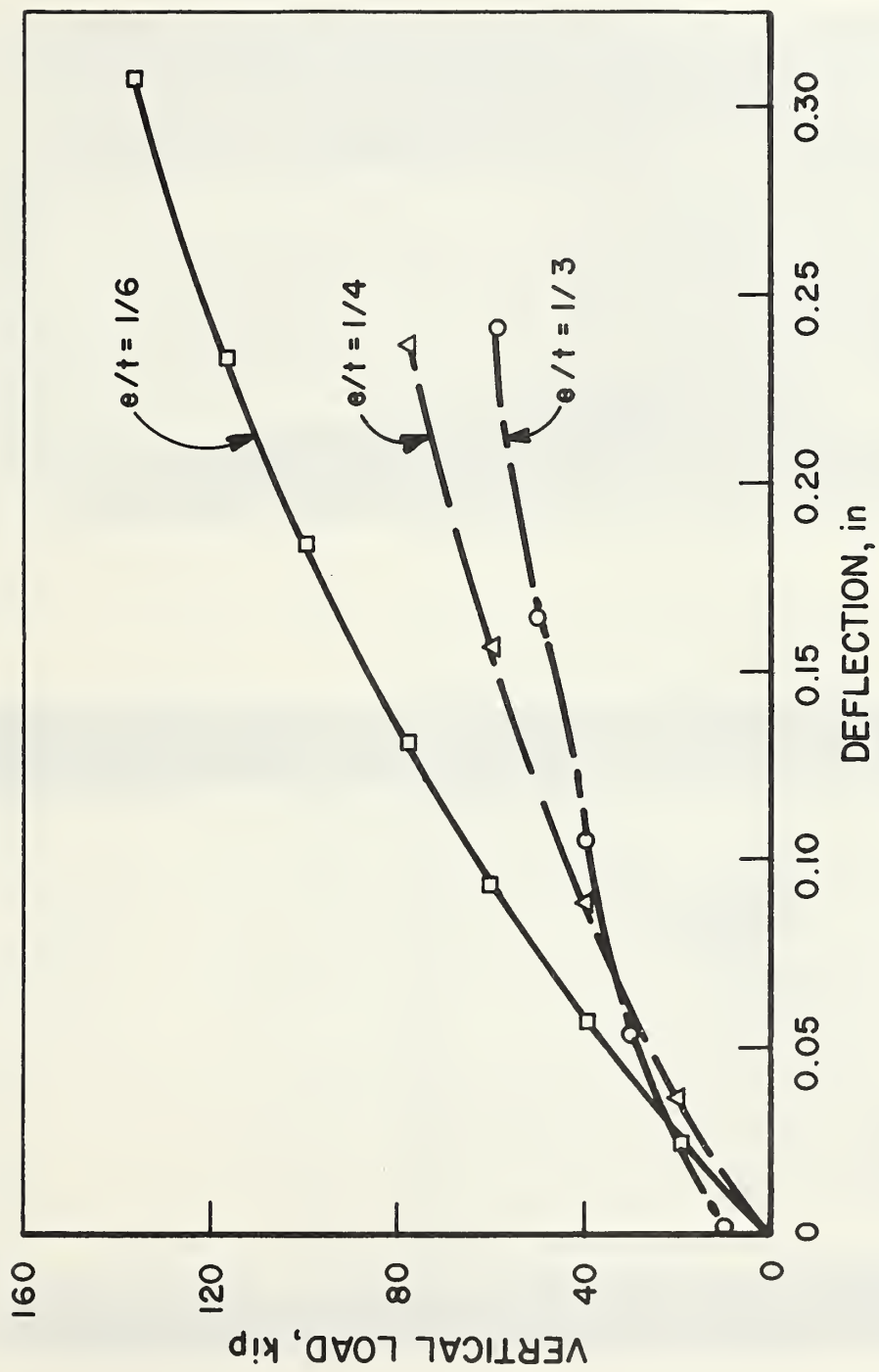
Table 5.1 Summary of 6-in Wall Test Results

Specimen Designation	No.	Age days	Eccentricity	in	Ultimate Load kip
10-R-0	1	30-32	0	0	354.8
10-R-0	2	29-31	0	0	328.0
10-R-0	3	11-12	0	0	361.8
10-R-0	4	14-15	0	0	369.4
10-R-T6	5	15-16	t/6	0.94	296.2
10-R-T6[a]	6	15-16	t/6	0.94	263.4
10-R-T4	7	14-18	t/4	1.41	247.3
10-R-T4	8	14-18	t/4	1.41	236.6
10-R-T3	9	14-15	t/3	1.88	189.8
10-R-T3	10	14-15	t/3	1.88	185.5
16-R-0	1	10-16	0	0	274.7
16-R-0	2	11-17	0	0	281.2
16-R-T6	3	7-13	t/6	0.94	212.9
16-R-T6	4	11-17	t/6	0.94	201.6
16-R-T4	5	8-14	t/4	1.41	170.4
16-R-T4	6	9-15	t/4	1.41	190.9
16-R-T3	7	7-9	t/3	1.88	146.8
16-R-T3	8	8-10	t/3	1.88	153.2
20-R-0	1	45-49	0	0	343.2
20-R-0	2	45-49	0	0	331.7
20-R-0	5	12-18	0	0	253.8
20-R-0[b]	6	7-13	0	0	184.4
20-R-T6	3	19-21	t/6	0.94	198.4
20-R-T6	4	19-21	t/6	0.94	202.0
20-R-T4	7	8-19	t/4	1.41	119.4
20-R-T4	8	9-20	t/4	1.41	129.0
20-R-T3	9	9-13	t/3	1.88	73.5
20-R-T3	10	10-14	t/3	1.88	83.9

[a] Bottom lintel block cracked during fabrication.

[b] Wall had a broken block on one end of the 8th course from the top.

LOAD-DEFLECTION CURVES FOR 16-FT REINFORCED WALLS
Fig. 5.3

LOAD-DEFLECTION CURVES FOR 20-FT REINFORCED WALLS

FIG. 5.4

Axially Loaded 10-ft Panel

Eccentrically Loaded 16-ft Panel

TYPICAL FAILURES OF 6-IN REINFORCED WALLS

Fig. 5.5

Table 5.2 Failures of 6-in Reinforced Walls

Wall Specimen Designation	No.	Age days	Description of Failure
10-R-0	1	30-32	Split down one side of one face about 1 unit from end. Failure occurred when top 1/4h came out.
10-R-T4	7	14-18	Top failed
10-R-T4	8	14-18	Failure in top 3 courses
10-R-T3	9	14-15	Failure in top 2 courses
16-R-0	1	10-16	Wall broke along horiz. joint 1/4h from top
16-R-0	2	11-17	Wall broke along horiz. joint 1/4h from top
16-R-T6	3	7-13	Wall broke along horiz. joint 1/4h from top
16-R-T6	4	11-17	Wall broke along horiz. joint 1/4h + from top
16-R-T4	5	8-14	Wall broke along horiz. joint between 4th & 5th course from top, compressive failure in 5th course.
16-R-T4	6	9-15	Wall broke along horiz. joint between 5th & 6th course from top.
16-R-T3	8	8-10	Failed at 6th course from top
20-R-0	1	45-49	Crushing of 7th course from top
20-R-0	5	12-18	Failure occurred in the 7th & 8th courses from the top. A large vertical crack developed at 214 kip in the instrumented part of the test. Crack extended from 18th to 24th course. There was no top reinforcement on west side of wall.
20-R-T6	3	19-21	Crushing between 6th & 7th courses from the top on the compression side of wall.
20-R-T6	4	19-21	Crushing between 6th & 7th course from the top on the compression side of wall. There was a slight bend in the wall about the top of the 15th course from the bottom.
20-R-T4	7	8-19	Wall slipped out of loading system with no apparent sign of failure, crushing bottom of 5th course from the top.
20-R-T4	8	9-20	Wall deflected considerably about 2 courses above bond beam (mid height) then slipped away from loading system. After failure had little residual deflection.
20-R-T3	9	9-13	Failure occurred by excessive bending at bottom of 7th course from the top.
20-R-T3	10	10-14	Large deflection prior to failure with greatest deflection 7th course from the top.

Deflections were considerably larger than in the 16-ft walls. At eccentricities of t/4 and t/3, the walls deflected excessively and tended to slip out of the loading system. These walls recovered after load removal and exhibited only small residual deflections. Most walls crushed at a horizontal joint 6 to 7 courses below the top of the wall.

5.2 8-in Unreinforced Walls

Wall test results are summarized in table 5.3 and plotted in figure 5.6. Figures 5.7 through 5.9 show load-deflection curves for the deflections at 3/4 height of the 8-in walls.

Wall failures are shown in figure 5.10. A log of all recorded individual failures is shown in table 5.4.

The 10-ft high walls failed in a manner resembling the failure of three-block high prisms. Axially loaded walls developed vertical cracks with final failure occurring by crushing between the second and fourth course from the top or bottom end of the wall at both wall faces. Eccentrically loaded walls failed between the top and the fourth course from the top by compressive failure on one wall

face at a mortar joint, except for one wall loaded at t/6 which failed near its base.

The 16-ft high walls generally failed along a horizontal joint at approximately 3/4 of their height. One axially loaded wall and one wall loaded at an eccentricity of t/6 failed by compression near the second course from the bottom of the wall.

Most 20-ft high walls also failed along a horizontal joint at approximately 3/4 of their height. One axially loaded wall and one with a load eccentricity of t/6 failed by crushing of the mortar joint three courses from the bottom.
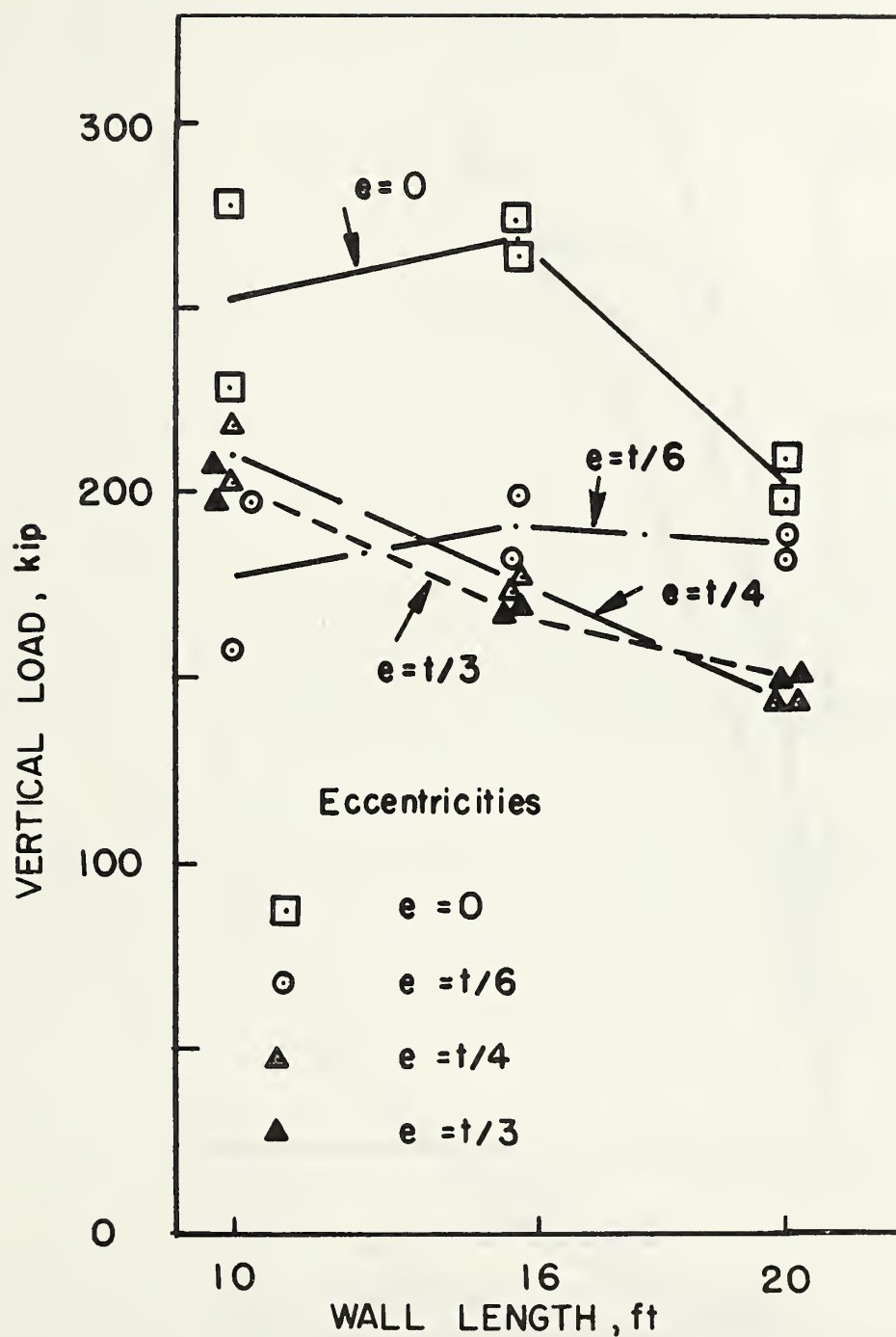
5.3. Prisms

Test results on eccentrically loaded 2-block high and 3-block high prisms made of 6-in and 8-in block are given in tables 5.5 and 5.6, respectively. These tables note the age, as well as the date of fabrication of prisms. This is important since it appears that the strength of prisms fabricated on certain dates sometimes tended to deviate markedly from the generally observed trend.

Table 5.3 Summary of 8-in Wall Test Results

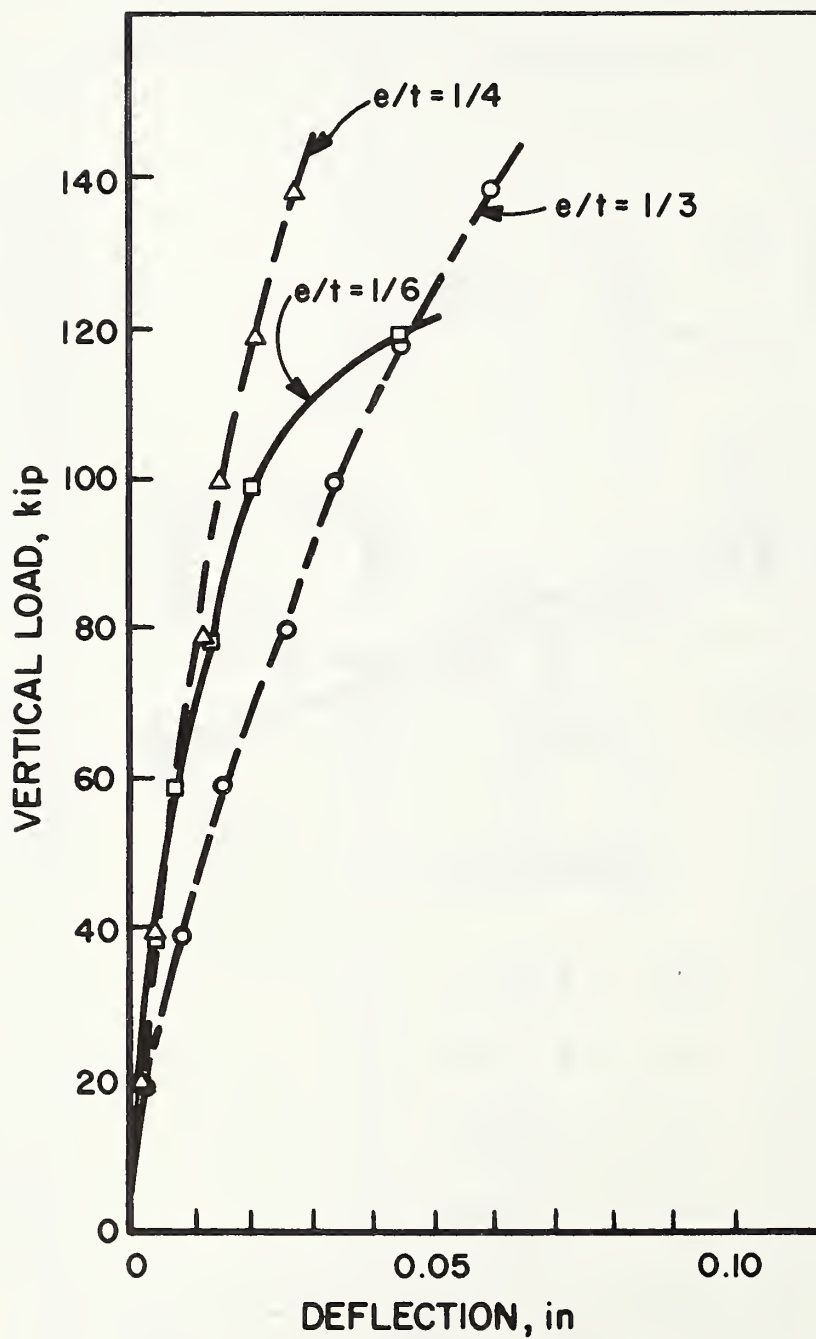| Specimen Designation	No.	Age days	Eccentricity	in	Ultimate Load kip
10-N-0	1	33-36	0	0	232.3
10-N-0	2	35-38	0	0	231.7
10-N-0[a]	3	16-18	0	0	170.4
10-N-0[a]	4	18-20	0	0	159.7
10-N-T6 [a] [b]	5	15	t/6	1.27	172.6
10-N-T6	6	18	t/6	1.27	166.1
10-N-T4	7	13-16	t/4	1.91	203.2
10-N-T4[b]	8	15-18	t/4	1.91	217.2
10-N-T3	9	13	t/3	2.54	198.4
10-N-T3	10	16	t/3	2.54	207.0
10-N-0	13	10-11	0	0	278.7
10-N-0	14	11-12	0	0	225.2
10-N-T6	11	12	t/6	1.27	157.4
10-N-T6	12	13	t/6	1.27	196.8
16-N-0	1	11-15	0	0	262.6
16-N-0	2	14-18	0	0	273.5
16-N-T6	3	14-15	t/6	1.27	199.7
16-N-T6	5	8-10	t/6	1.27	181.7
16-N-T4	4	14-15	t/4	1.91	175.3
16-N-T4	6	11-13	t/4	1.91	172.0
16-N-T3	7	10-11	t/3	2.54	166.1
16-N-T3	8	11-12	t/3	2.54	169.4
20-N-0	1	39-44	0	0	233.5
20-N-0	2	39-44	0	0	249.2
20-N-0	3	22	0	0	195.8
20-N-0	6	12-13	0	0	208.1
20-N-T6	4	22	t/6	1.27	188.7
20-N-T6	5	12-13	t/6	1.27	180.2
20-N-T4	7	14-15	t/4	1.91	143.0
20-N-T4	8	14-15	t/4	1.91	143.0
20-N-T3	9	8-10	t/3	2.54	148.1
20-N-T3	10	8-10	t/3	2.54	150.5

[a] Walls had some mortar joints of thickness in excess of
3/8-in.

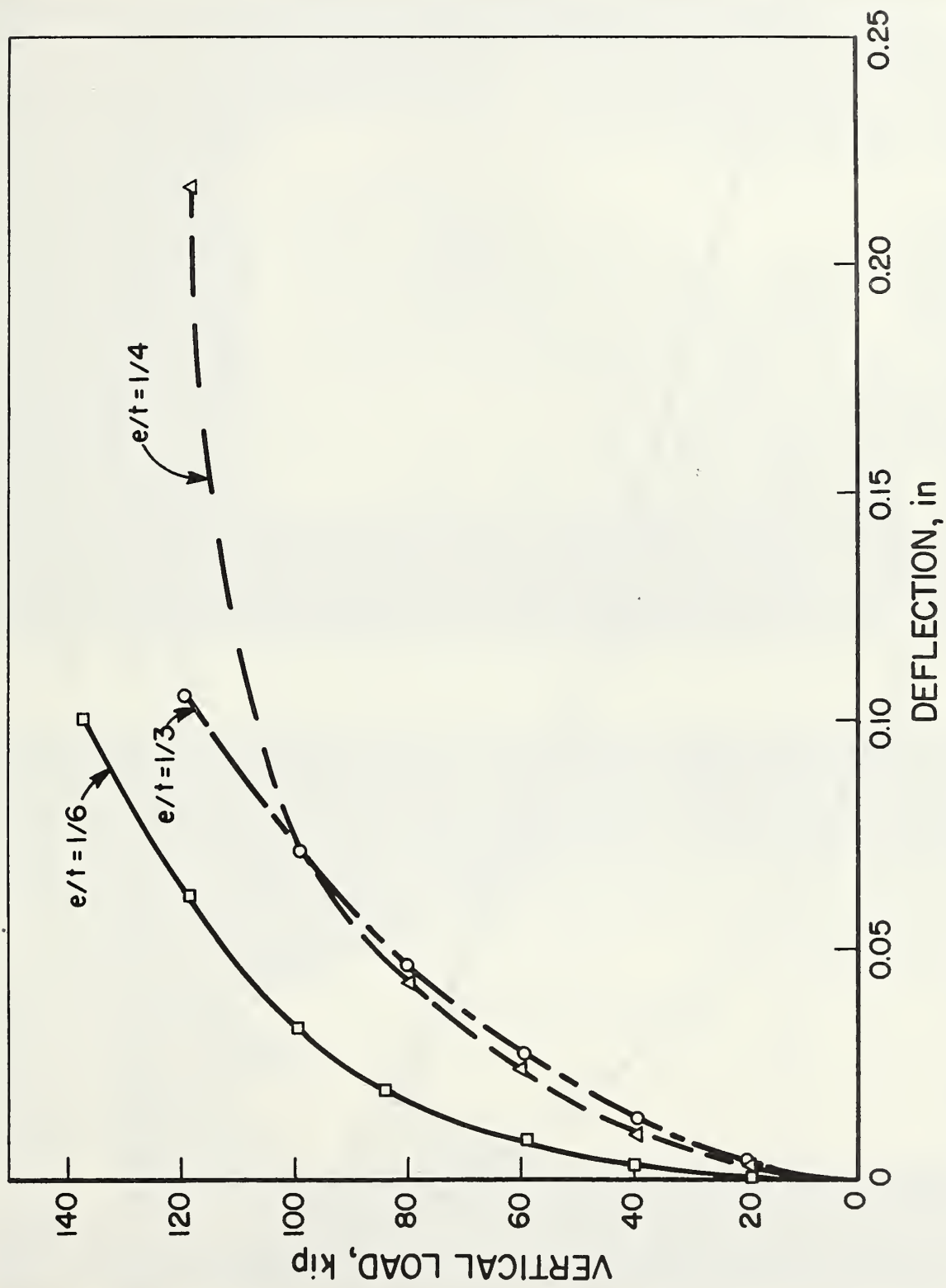[b] Wall was damaged by the yoke used in transporting it.
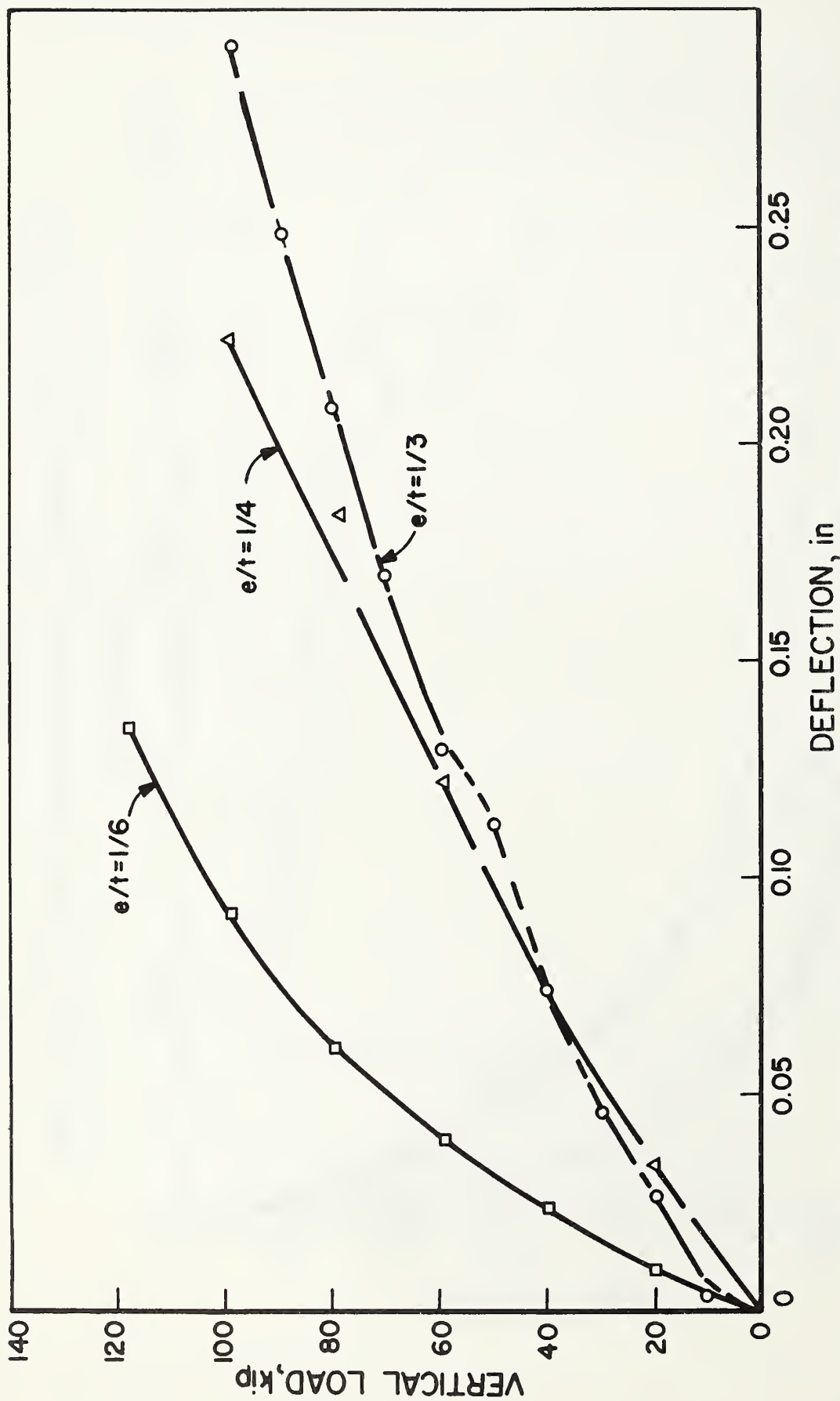
FAILURE LOADS FOR 8-IN UNREINFORCED WALLS

Fig. 5.6

LOAD-DEFLECTION CURVES FOR
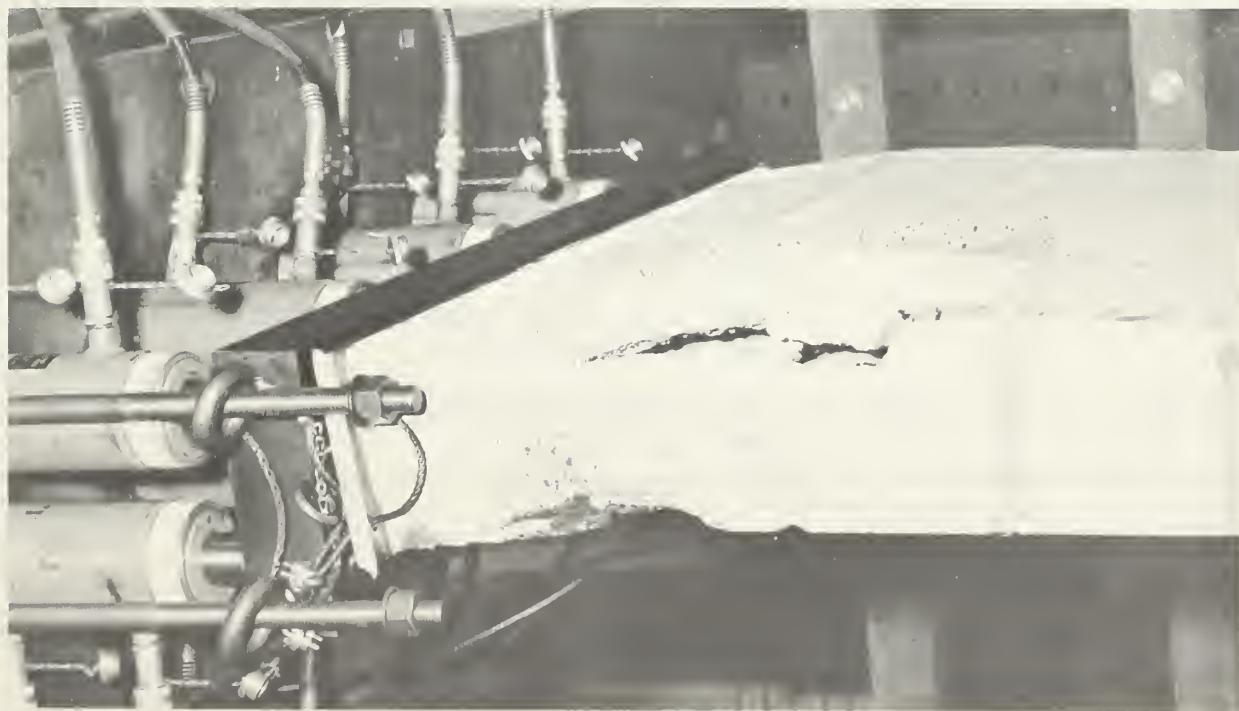IO-FT UNREINFORCED WALLS

Fig. 5.7

LOAD-DEFLECTION CURVES FOR 16-FT UNREINFORCED WALLS

Fig.5.8

LOAD-DEFLECTION CURVES FOR 20-FT UNREINFORCED WALLS

Fig. 5.9

TYPICAL FAILURES OF 8-IN UNREINFORCED WALLS
Fig. 5.10

TABLE 5.4

Failures of 8-in Unreinforced Walls

Wall Specimen			Description of Failure
Designation	No.	Age, days	
10-N-0	1	33-36	Wall split through center vertically to bottom 1/4h where it broke down and out to bottom corners. Typical compression failure of block.
10-N-0	2	35-38	Compression failure in 2nd course from bottom.
10-N-0	3	16-18	Vertical splitting and cracking in the shape of an inverted V at top 1/4h point of wall.
10-N-T4	7	13-16	Bending with subsequent compression failure in mortar joint at yoke location (top of 9th course).
10-N-T3	·9	13	Bending in the wall, compressive failure in the mortar joint on inside of bend and sudden rupture.
10-N-T3	10	16	Bending and subsequent failure at the mortar joint between 3rd and 4th courses from the top.
10-N-T6	11	12	Splitting of 1st and 2nd course from the bottom.
16-N-0	1	11-15	Wall broke about 1/4h from top along a horizontal joint and blew out.
16-N-0	2	14-18	Compression failure in 2nd course from bottom, wall broke up and fell straight down.
16-N-T6	3	14-15	Compression failure in 1st and 2nd course from bottom, wall broke along horizontal joint 1/4h from bottom.
16-N-T6	5	8-10	Wall broke along horizontal joint between 1/3h and 1/4h from the top.
16-N-T4	4	14-15	Wall broke along horizontal joint 1/4h from the top.

Table 5.4 continued

Wall Specimen			Description of Failure
Designation	No.	Age, days	
16-N-T4	6	11-13	Failure originated at 2nd course from top and wall fell sideways.
16-N-T3	8	11-12	Failed at 6th joint from top
20-N-0	1	39-44	Failure 5th course from the top - 2/3 way through test vertical cracking in 2nd and 3rd courses from bottom.
20-N-0	3	22	Failed near the top.
20-N-0	6	12-13	Crushing about 3rd course from the bottom.
20-N-T6	4	22	Failure occurred 5th course from top along horizontal joint
20-N-T6	5	12-13	Failure in mortar joint 3rd course from the bottom.
20-N-T4	7	14-15	Failure occurred 1/4h from top, very little deflection was visible prior to failure.
20-N-T4	8	14-15	Failure occurred about 1/5h from the top.
20-N-T3	9	8-10	Failure occurred near 7th course from the top.
20-N-T3	10	8-10	Spalling at 2nd course from top. Failure at 6th course from top.

TABLE 5.5

Summary of 6-in Prism Test Results

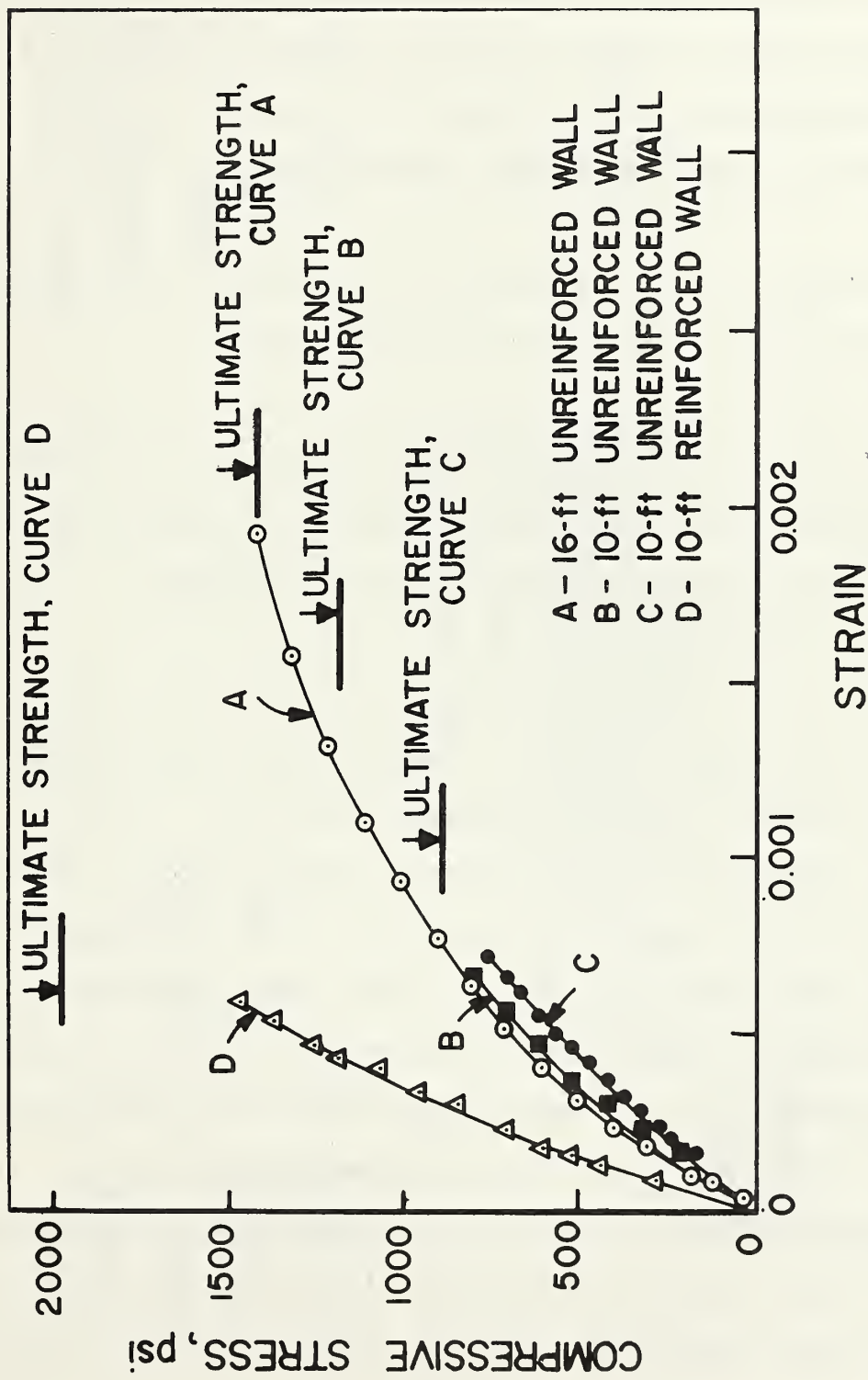| Prism Designation	Height	Eccentricity	Eccentricity in	Age days	Maximum Load kip	Average Maximum Load kip	Date of Construction
6-2-0	2-block	0	0	31	77.4	85.2	7/11
6-2-0	2-block	0	0	28	93.0		7/16
6-2-0	2-block	0	0	13	80.6		7/31
6-2-0	2-block	0	0	9	81.2		7/9
6-2-0	2-block	0	0	11	69.6	76.5	9/15
6-2-0	2-block	0	0	11	76.4		9/15
6-2-0	2-block	0	0	11	74.5		9/15
6-2-T6	2-block	t/6	0.94	9	74.0	73.3	7/31
6-2-T6	2-block	t/6	0.94	9	72.6		8/6
6-2-T4	2-block	t/4	1.41	9	76.0		8/12
6-2-T4	2-block	t/4	1.41	10	112.0	85.1	9/3
6-2-T4	2-block	t/4	1.41	11	67.4		9/15
6-2-T3	2 block	t/3	1.88	9	63.8		8/6
6-2-T3	2 block	t/3	1.88	7	84.2	77.0	9/6
6-2-T3	2 block	t/3	1.88	9	83.0		8/12
6-3-0	3-block	0	0	29	82.3	84.9	7/11
6-3-0	3-block	0	0	29	87.6		7/16
6-3-0	3-block	0	0	14	81.3		7/31
6-3-0	3-block	0	0	9	58.7		7/9
6-3-0	3-block	0	0	9	90.4	79.5	8/12
6-3-0	3-block	0	0	11	77.6		9/15
6-3-0	3-block	0	0	11	89.5		9/15
6-3-T6	3-block	t/6	0.94	8	61.0	61.8	8/6
6-3-T6	3-block	t/6	0.94	8	62.5		8/6
6-3-T4	3-block	t/4	1.41	9	72.6		8/12
6-3-T4	3 block	t/4	1.41	11	63.0	81.6	9/15
6-3-T4	3 block	t/4	1.41	7	109.2		9/6
6-3-T3	3-block	t/3	1.88	9	78.6		8/12
6-3-T3	3-block	t/3	1.88	7	85.0	81.8	9/6

TABLE 5.6

Summary of 8-in Prism Test Results

Prism Designation	Height	Eccentricity	Eccentricity in	Age days	Maximum Load kip	Average Maximum Load kip	Date of Construction
8-2-0	2-block	0	0	28	109.5	108.5	7/17
8-2-0	2-block	0	0	28	107.5		7/18
8-2-0	2-block	0	0	14	77.0		7/1
8-2-0	2-block	0	0	13	87.6		7/2
8-2-0	2-block	0	0	12	75.2	84.6	7/31
8-2-0	2-block	0	0	12	71.0		7/31
8-2-0	2-block	0	0	11	112.0		9/15
8-2-T6	2-block	t/6	1.27	15	82.6	77.3	7/2
8-2-T6	2-block	t/6	1.27	12	72.0		7/17
8-2-T4	2-block	t/4	1.91	13	69.3		7/18
8-2-T4	2-block	t/4	1.91	13	71.0	75.0	7/18
8-2-T4	2-block	t/4	1.91	9	84.6		8/12
8-2-T3	2-block	t/3	2.54	11	72.0		9/15
8-2-T3	2-block	t/3	2.54	8	60.6	71.4	7/29
8-2-T3	2-block	t/3	2.54	19	58.5		8/6
8-2-T3	2-block	t/3	2.54	9	94.6		8/12
8-3-0	3-block	0	0	28	78.3		7/18
8-3-0	3-block	0	0	31	101.0	89.0	7/17
8-3-0	3-block	0	0	29	87.6		7/17
8-3-0	3-block	0	0	14	.87.8		7/1
8-3-0	3-block	0	0	13	89.2	96.4	7/2
8-3-0	3-block	0	0	11	117.0		9/15
8-3-0	3-block	0	0	11	91.5		9/15
8-3-T6	3-block	t/6	1.27	14	64.7		7/17
8-3-T6	3-block	t/6	1.27	11	62.6	65.0	7/18
8-3-T6	3-block	t/6	1.27	15	67.8		
8-3-T4	3-block	t/4	1.91	13	56.9		7/18
8-3-T4	3-block	t/4	1.91	13	58.2	60.1	7/18
8-3-T4	3-block	t/4	1.91	9	65.2		8/12
8-3-T3	3-block	t/3	2.54	15	53.4		7/29
8-3-T3	3-block	t/3	2.54	14	48.3	57.7	7/30
8-3-T3	3-block	t/3	2.54	9	71.6		8/12

6.1 Stress-Strain Relationships

Stress-strain relationships, measured on unreinforced as well as reinforced walls, are shown in figure 6.1. Curve A shows a stress-strain curve computed from the longitudinal deformation of an axially loaded 16-ft unreinforced wall (specimen 2). This is the only case where deflections were measured to the point of ultimate load. In all other cases instrumentation was removed prior to failure. Curves B and C are stress-strain curves for axially loaded 10-ft unreinforced walls, computed from the average of measurements of 4 linear variable differential transducers having a gage length of 24-in, which were specially installed for that purpose. (Curve B is for specimen 14 and curve C for specimen 4.) Curve C was obtained from one of the specimens with excessive joint thickness and may therefore represent a wall of lower-than-normal strength. The ultimate compressive strength of the specimens from which curves B and C were derived is also shown in the figure. Stress was computed on the basis of the average net area, determined in accordance with ASTM Standard C140-65T.

There is good agreement between the three curves. However, Curve A, which is the only curve that covers stress-strain

STRESS-STRAIN CURVES

FIG. 6.1

relations to the point of failure, was derived from a
specimen of higher-than-average strength. In general the
stress-strain curves are not linear, however, it appears
that up to the strength achieved by most specimens under
pure compression, stress-strain relationships could be
reasonably approximated by a linear curve.

The following values of moduli of elasticity were experi-
mentally derived for the unreinforced walls:

Initial modulus of elasticity, E_i = 1.4 x 10^6 psi.
Approximate final tangent modulus of elasticity
at the stress level of most wall failures,
E_t = 0.4 x 10^6 psi.

Curve D in figure 6.1 shows stress-strain relationships
for an axially loaded reinforced 10-ft wall. In this
case, stresses were determined on the basis of the trans-
formed section shown in figure 6.2. This transformed
section was developed using a "net" cross sectional area
for the block which is based on minimum face-shell and
web thicknesses, the area of the grout and a transformed
steel area based on an "n" of 29 assuming that the
average modulus of elasticity of masonry is approximately
1 x 10^6 psi and that of steel is 29 x 10^6 psi. It can be
seen from a comparison of curve D with curves A, B and C

50

TRANSFORMED AREAS

MASONRY : 128

GROUT : 46

STEEL : 17

TOTAL 191 in²

MASONRY: E = 1 x 10⁶ psi

STEEL: E = 29 x 10⁶ psi

FOR STEEL: $n = \dfrac{E_s}{E_m} = 29$

FOR GROUT n = 1

1.0"

5.625"

3.625"

1.0"

6.3125"

6.3125"
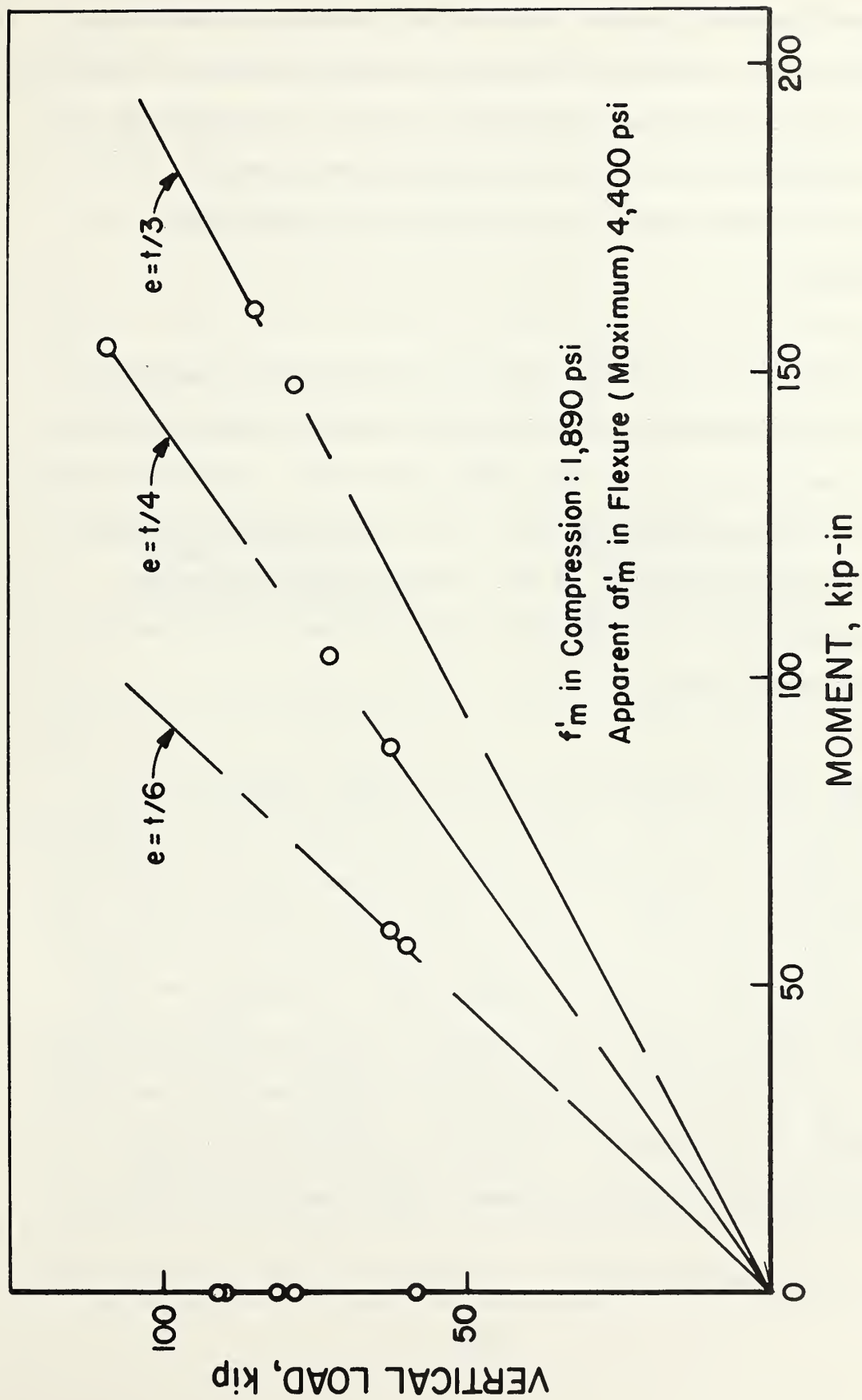
9.0"

21.625"

47.625"

17.4 in²

STEEL
GROUT
MASONRY

ASSUMED TRANSFORMED AREA FOR REINFORCED MASONRY WALL

FIG. 6.2

that the area transformation which conservatively assumed
equal stiffness for grout and masonry and also was based
on mimimum, rather than average net area of masonry prob-
ably resulted in overestimating the stresses in the ma-
sonry. Further research should be conducted to determine
the interaction of the component materials in reinforced
masonry.

The value of the initial modulus of elasticity derived
from curve D is 2.8 x 10^6 psi. A tangent modulus at
failure could not be obtained since instrumentation was
removed before the masonry developed its ultimate strength.
Note that the stress-strain curve is essentially linear
up to a stress of about 80% of the failure stress. A
linear stress-strain relationship probably approximates
the stress distribution up to failure reasonably well.

6.2 Cross-Sectional Capacity

In order to study the capacity of slender walls, it is
first necessary to consider the strength of short wall
sections. Figure 6.3 shows a plot of the failure loads
of eccentrically loaded three-block high 6-in prisms.
Loads were applied axially and at eccentricities of t/6,
t/4 and t/3. Note that even though there is considerable
scatter between individual test points no trend can be

6-IN HOLLOW BLOCK PRISMS UNDER ECCENTRIC LOADING

Fig.6.3

observed for the failure load to decrease with increasing
eccentricity. Similar behavior have been observed elsewhere
for solid sections of concrete as well as clay-masonry [8].
It is apparent that flexural compressive strength of ma-
sonry increases significantly with increasing strain
gradients.

The 6-in block of which prisms were tested were used in
the construction of the reinforced masonry walls. However,
these walls also contained grout and steel, and the section
capacity of a reinforced wall will depend on the strength
and relative stiffness of all the component materials.
The correlation between prism strength and wall strength
is discussed below.

Average axial compressive prism strength computed from
the 6-in prism tests, based on minimum net area is 1890 psi.
This stress, multiplied by the transformed area shown in
figure 6.2 (191 in^2) results in a computed axial failure
load of 361 kip. This compares with an average 366-kip
failure load for the 10-ft axially loaded reinforced walls.
Thus the 10-ft walls approximately developed the predicted
ultimate axial strength. This is a good correlation,
considering the scatter between individual test points.

It is somewhat more difficult to compare flexural com-
pressive strength, since at each eccentricity the 6-in
prisms developed different flexural compressive strength,
with an apparent increase in strength with increasing
strain gradients. Average flexural compressive strengths
developed at an eccentricity of t/3 by the 6-in prisms
and by the 10-ft reinforced walls respectively, are com-
pared below. The transformed section in figure 6.2 was
used to compute stresses in the reinforced walls.

Average flexural
strength of 6-in
prisms, at t/3 eccen-
tricity: 4,400 psi.

Average flexural
strength of 10-ft
walls, at t/3 eccen-
tricity: 2,900 psi.

Stresses were computed for a linear stress distribution.
While the 6-in prisms developed flexural compressive
strength which exceeded the strength under axial loading
by as much as 130%, the strength increase in the case of
the wall was only 50%. Thus, there is good correlation
between wall strength and prism strength under axial
loading, while under eccentric loading the prisms developed
higher flexural compressive strength than the walls. The
question arises whether the strength of the 10-ft wall
was reduced by slenderness effects. The failure mode of
these walls indicates that they failed near the top, where
the eccentric load was applied. It will be explained

later that this is an indication that slenderness had no significant effect on wall strength. The discrepancy between flexural strength of prisms and walls is probably caused by composite action of the wall rather than slenderness effects.

Figure 6.4 shows the failure loads of the 10-ft high reinforced walls, plotted against applied moments (load x eccentricity). Test points for individual specimens are numbered in accordance with table 5.1. If it is assumed that the strength of the 10-ft walls was not appreciably affected by slenderness, this plot also represents the cross sectional capacity of these walls. The solid curve shown in the figure is a theoretical interaction curve for the section capacity of this wall. Moments were computed on the assumption that at failure plane sections remain plane and that the stress distribution was approximately linear. The transformed section in figure 6.2 was used in the computations. The yield strength of the steel, f'_s, was taken as 60,000 psi, and f'_m, the compressive strength of masonry, was computed from the average prism strength under axial load as 1890 psi. Additional information pertaining to the development of theoretical interaction curves is contained in reference [8].

It can be seen by comparing the actual test results with

56

f'$_m$ Compression : 1,890 psi
Apparent a f'$_m$ in Flexure at
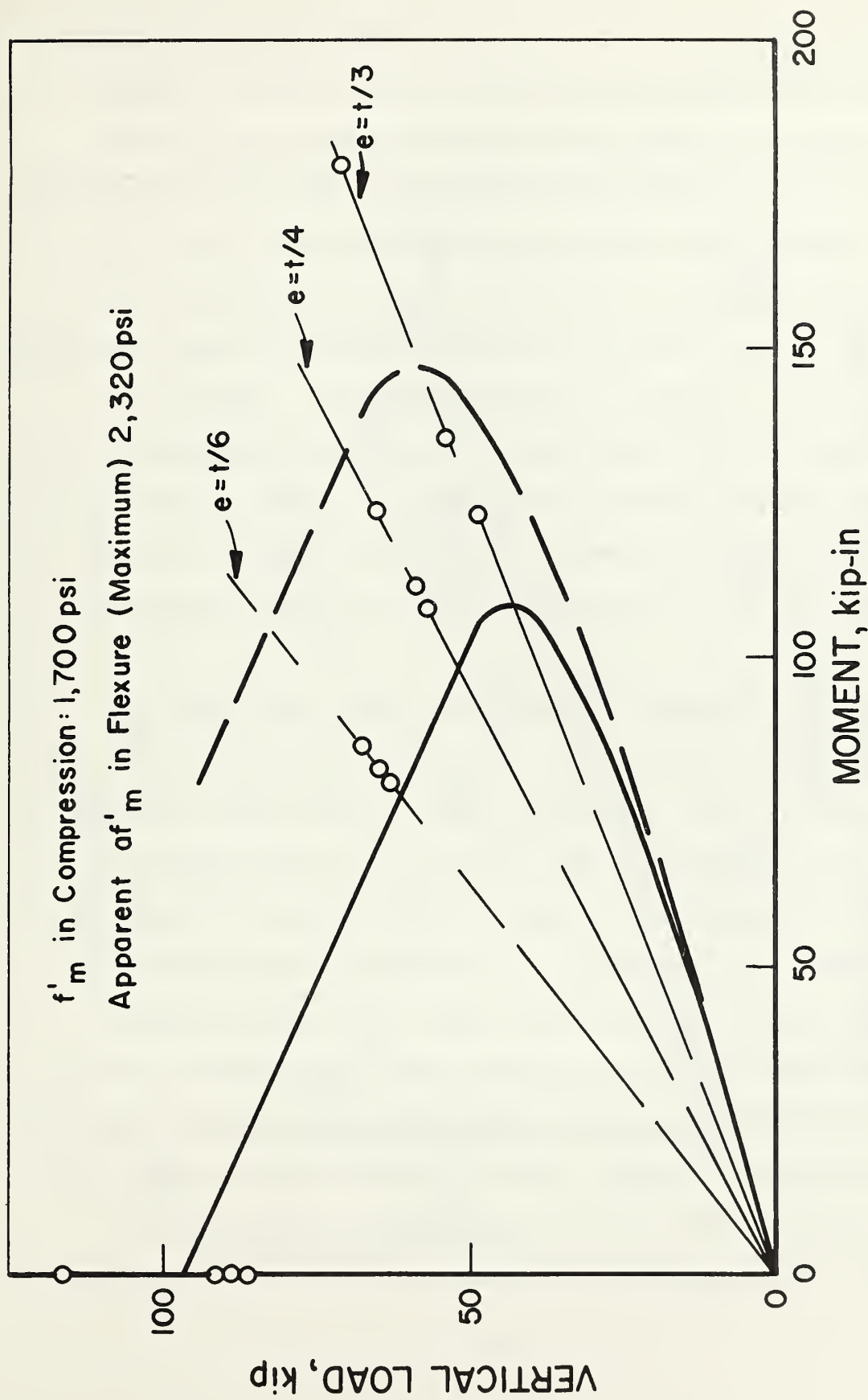Maximum Eccentricity 2,900 psi

SHORT-WALL INTERACTION-CURVE AND TEST RESULTS
FOR 10-FT HIGH REINFORCED MASONRY WALLS

Fig. 6.4

the intersection points of the solid interaction curve
with the dashed sloping lines representing the various
load eccentricities of the tests that moment capacities
are very conservatively predicted. Another interaction
curve has been computed, using the average flexural com-
pressive strength developed by the walls at the maximum
test eccentricity of t/3, which is 2900 psi. This curve
is shown by the dashed line in figure 6.4. Note that this
curve agrees with actual test results only at the t/3
eccentricity. At smaller eccentricities the curve over-
estimates wall strength, and it is apparent by the way the
curve diverges from the test results that flexural strength
increased with increasing eccentricity. If this observation
is extrapolated to eccentricities greater than t/3, it may
be deduced that the curve is conservative for eccentricities
greater than t/3, but overestimates moment capacities for
eccentricities smaller than t/3. If we define flexural
strength as af'_m, where a is a function of load eccentricity
(or strain gradients), then for the test results of the
reinforced walls at t/3 eccentricity $a \approx 1.5$.

Figure 6.5 shows a plot of the failure loads of three-
block high 8-in prisms subjected to axial and eccentric
vertical loads. Again an interaction curve was computed
on the basis of average axial compressive strength,
f'_m = 1700 psi. This curve is represented by the solid

58

f'_m in Compression : 1,700 psi

Apparent af'_m in Flexure (Maximum) 2,320 psi

e = t/6

e = t/4

e = t/3

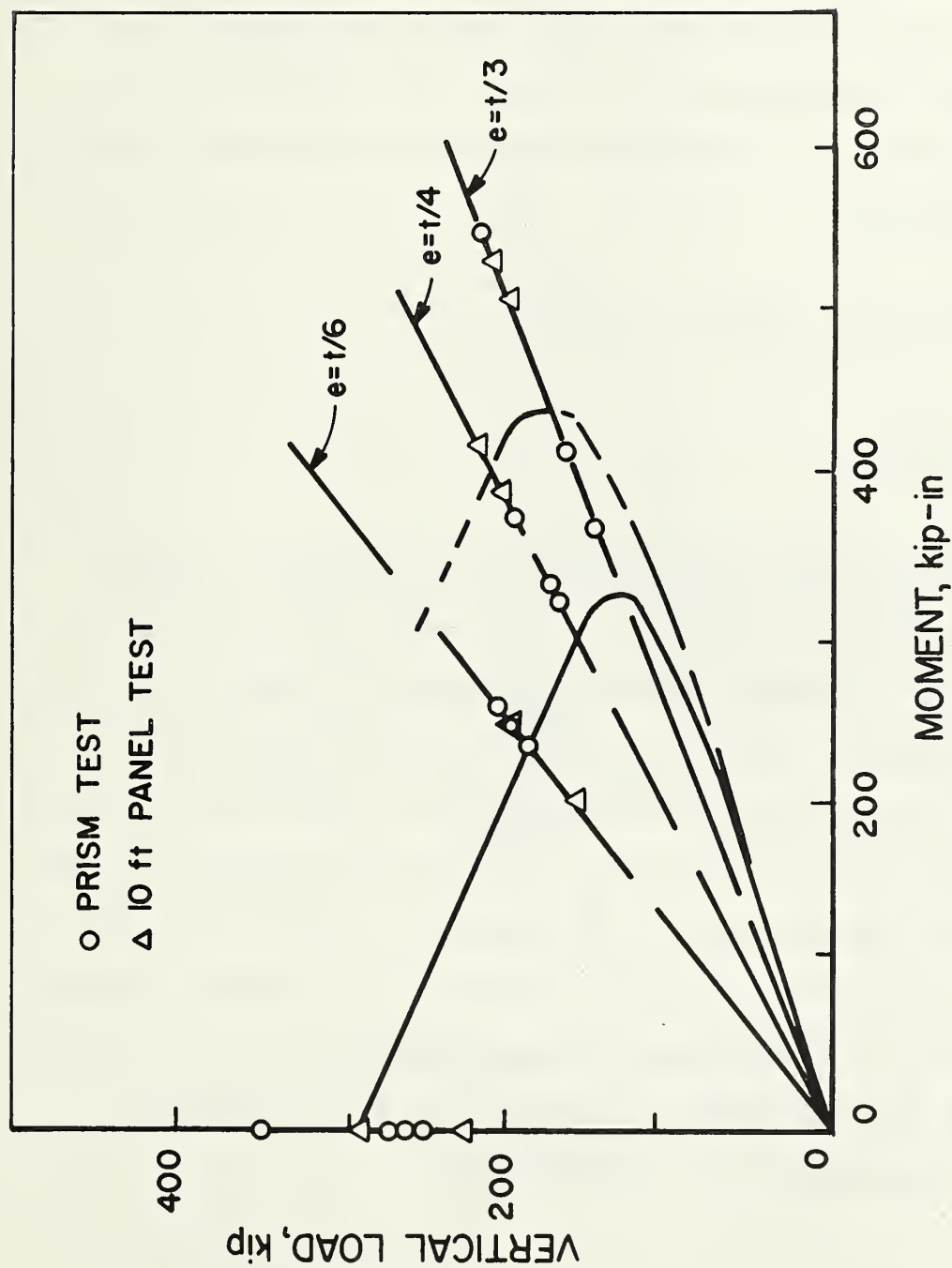VERTICAL LOAD, kip

MOMENT, kip-in

8-IN HOLLOW BLOCK PRISMS UNDER ECCENTRIC LOADING

Fig. 6.5

curve in figure 6.5. It can be seen that moment capacities
are very conservatively predicted by this curve. Another
interaction curve has been developed on the basis of the
average flexural compressive strength at the t/3 eccentricity
and is shown in the figure by the dashed curve. As in the
case of the reinforced walls this curve diverges from the
trend of the test results at smaller eccentricities, indicating
that "a" is a function of strain gradients. Again it may
be deduced that the dashed curve is probably conservative
for load eccentricities greater than t/3, while overesti-
mating capacities for smaller load eccentricity. In this
case af'_m at the t/3 eccentricity is 2,320 psi and $a \simeq 1.37$.

A comparison of prism strength with 10-ft wall panel
strength is shown in figure 6.6. The interaction curves for
a = 1 and a = 1.37, developed from the prism data, are also
plotted in the figure. Note that at the larger eccen-
tricities average wall strength exceeded prism strength,
while under axial loading and at the t/6 eccentricity wall
strength tended to be somewhat lower than prism strength.
A comparison of all the eccentric wall tests seems to show
no noticeable effect of the magnitude of load eccentricity
on failure load, however, there is considerable scatter in
experimental results at axial load and at the t/6 eccen-
tricity. In general there appears to be no trend for the

60

COMPARISON OF PRISM STRENGTH AND 10-FT
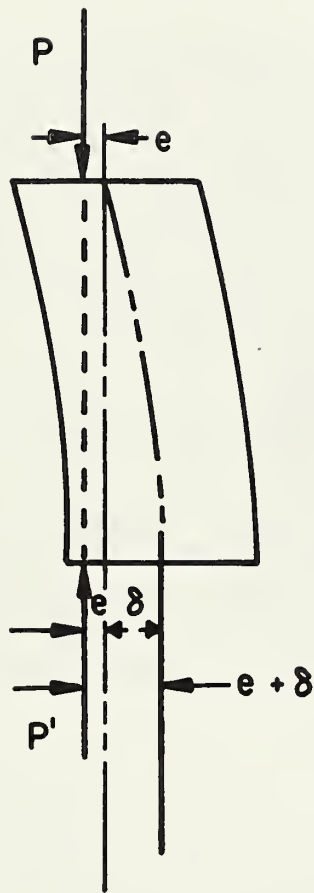PANEL STRENGTH FOR UNREINFORCED WALLS

Fig. 6.6

section capacity to decrease at this wall height. The
interaction curve developed on the basis of axial strength
is, in general, conservative for eccentric loads, however,
one wall test each at axial load and at t/6 eccentricity
falls below the predicted strength. This appears to be
caused primarily by strength variations between individual
test specimens.

6.3 Slenderness Effects

6.3.1 General

Slenderness effects are illustrated in figure 6.7 which
shows the free body diagram of the upper part of a wall,
subject to a vertical load P applied at its top at an
eccentricity e. The free body is in equilibrium when
force P is resisted at the bottom of the free body by the
resultant colinear force P'. If the wall deflected at the
bottom of the free body by an amount δ relative to the
line of action of the vertical force, the resisting moment
acting at the base of the free body will be $P(e + \delta)$, and
thus the external moment acting at the top of the wall
will be magnified by the amount $P \cdot \delta$.

62

SLENDERNESS EFFECTS

Fig.6.7

It has been shown [9] that for the case of reinforced concrete columns the maximum moment can be approximately computed by the following equation:

$$M = Pe \; \frac{C_m}{1 - \dfrac{P}{P_{cr}}} \; \geq \; Pe \tag{1}$$

where C_m is a correction factor, relating different moment distributions to the basic case of a pin ended column acted upon by a vertical load at equal eccentricities at the top and the bottom, ($C_m = 1$ for this case) and

$$P_{cr} = \frac{\pi^2 EI}{(kh)^2} \tag{2}$$

is the axial load that will cause stability induced compression failure. "k" in the term kh is a "length coefficient", by which height is adjusted to equivalent height, accounting for end support conditions.

In the case of masonry walls a similar mechanism will cause a decrease in wall strength with increasing wall slenderness. Inspection of the wall failure descriptions in tables 5.2 and 5.4 reveals a general trend for the more slender walls to fail in flexure along a horizontal joint in the vicinity of the point of maximum deflection, while shorter walls tended to fail near the top where the eccentricity of the

64

applied load relative to the undeflected wall is greatest.
However, the magnitude of this moment magnifier effect in
the case of masonry walls depends on several parameters:

1) End Fixity: The flat ended condition of these
tests appears to resemble fixed ended conditions. However,
previous experience with similar conditions in brick walls
[10] indicates, that while the effect of eccentrically
applied loads can be approximately predicted by eq(1) for
pin ended conditions (even in the case of double curvature),
wall strength was overestimated when it was assumed that
flat ended walls similar to those in this investigation are
fixed ended. Assumptions made with respect to end conditions
are discussed in the following section.

2) Stiffness: The stiffness EI, in the case of
masonry, is subject to change with the magnitude and dis-
tribution of stresses that act on the cross section.
Both E and I depend on the moment distribution at failure;
E decreases with increasing stresses, as can be seen in
curve A in figure 6.1 while I decreases with section cracking.
Since greater deflections and smaller failure loads are
associated with greater eccentricities and slenderness,
more section cracking takes place with a corresponding de-
crease in stiffness. It has been shown for concrete columns
[9] that slenderness effects can be approximately predicted

by using an "equivalent EI":

$$EI = \frac{E_i I_n}{2.5} \qquad (3)$$

where E_i = Initial tangent modulus of elasticity,

$\quad\quad I_n$ = Moment of inertia of section based on uncracked net section.

However, this equation is valid in a range of loads and eccentricities where section cracking is not very significant.

For the case of brick masonry, slenderness effects have been approximately predicted [8] by the following equation:

$$EI \simeq E_i I_n \left(0.2 + \frac{P}{P_o}\right) \leq 0.7\; E_i I_n$$

where P_o = Short wall axial load capacity determined on the basis of prism strength.

or for low vertical loads:

$$EI = \frac{E_i I_n}{3}$$

In the interpretation of test results of this investigation eq(3) was used for the reinforced walls, assuming that reinforced masonry and reinforced concrete have similar properties. For unreinforced walls the reduction was based on the observation that the initial tangent modulus of elasticity equals about 3.5 times the modulus of elasticity at failure. Thus the "equivalent EI" was taken as:

$$EI = \frac{E_i I_n}{3.5} \qquad (4)$$

6.3.2 6-in Reinforced Walls

(1) End fixity: End conditions are related to the shape of deflection curves. Figure 6.8 shows measured deflection curves for the 10-ft, 16-ft and 20-ft reinforced walls. The curves for the 10-ft walls seem to indicate that there was only a minor amount of end fixity in spite of the flat-ended condition. The great stiffness of these walls and the relatively minor amount of rotation associated with a significant loss in end stiffness are probably contributing factors to the loss of end fixity. The 16-and 20-ft walls show a much more pronounced effect of end fixity. Average conditions of base fixity which were assumed for the 16- and 20-ft walls are illustrated in figure 6.9. These conditions correspond to the following end moments:

$$M_1 = Pe \qquad\qquad M_2 = -1/4\ Pe$$

$$M_2/M_1 = -1/4$$

In accordance with reference [9], this condition would correspond to the following values of C_m and k:
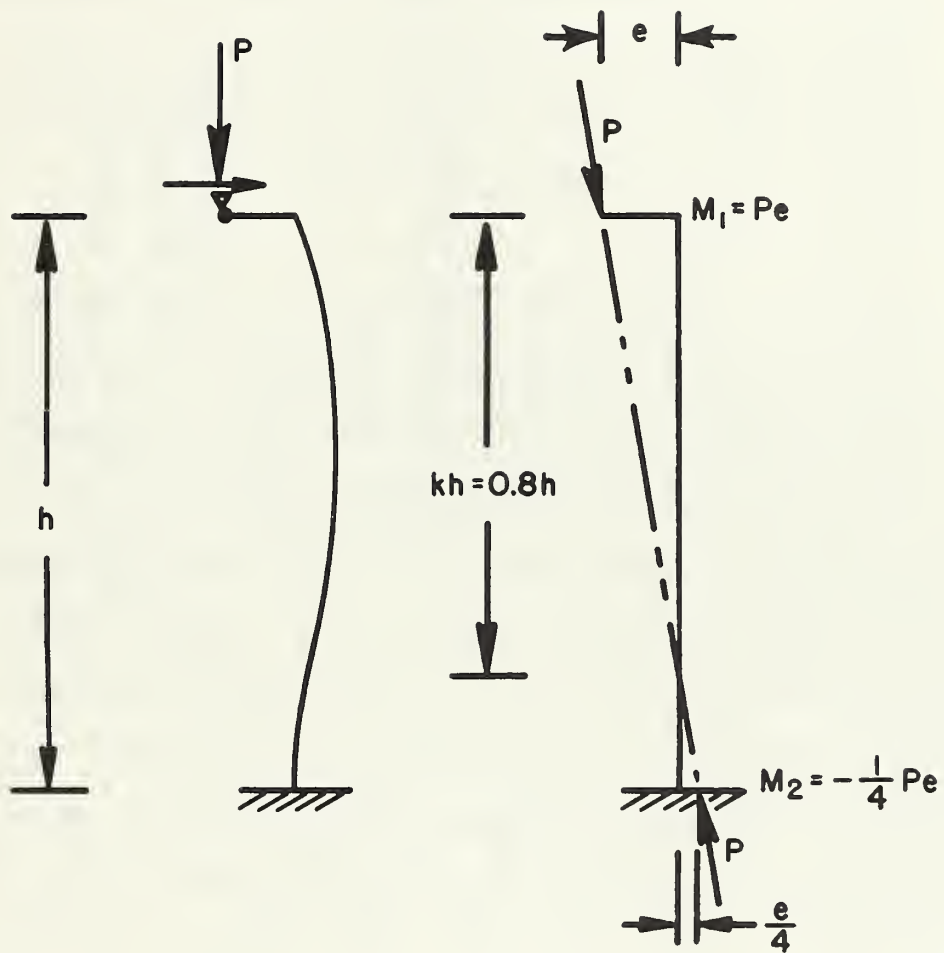
$$C_m = 0.6 + 0.4\ (-1/4) = 0.5$$

$$k = 0.8$$

67

TYPICAL DEFLECTION CURVES FOR
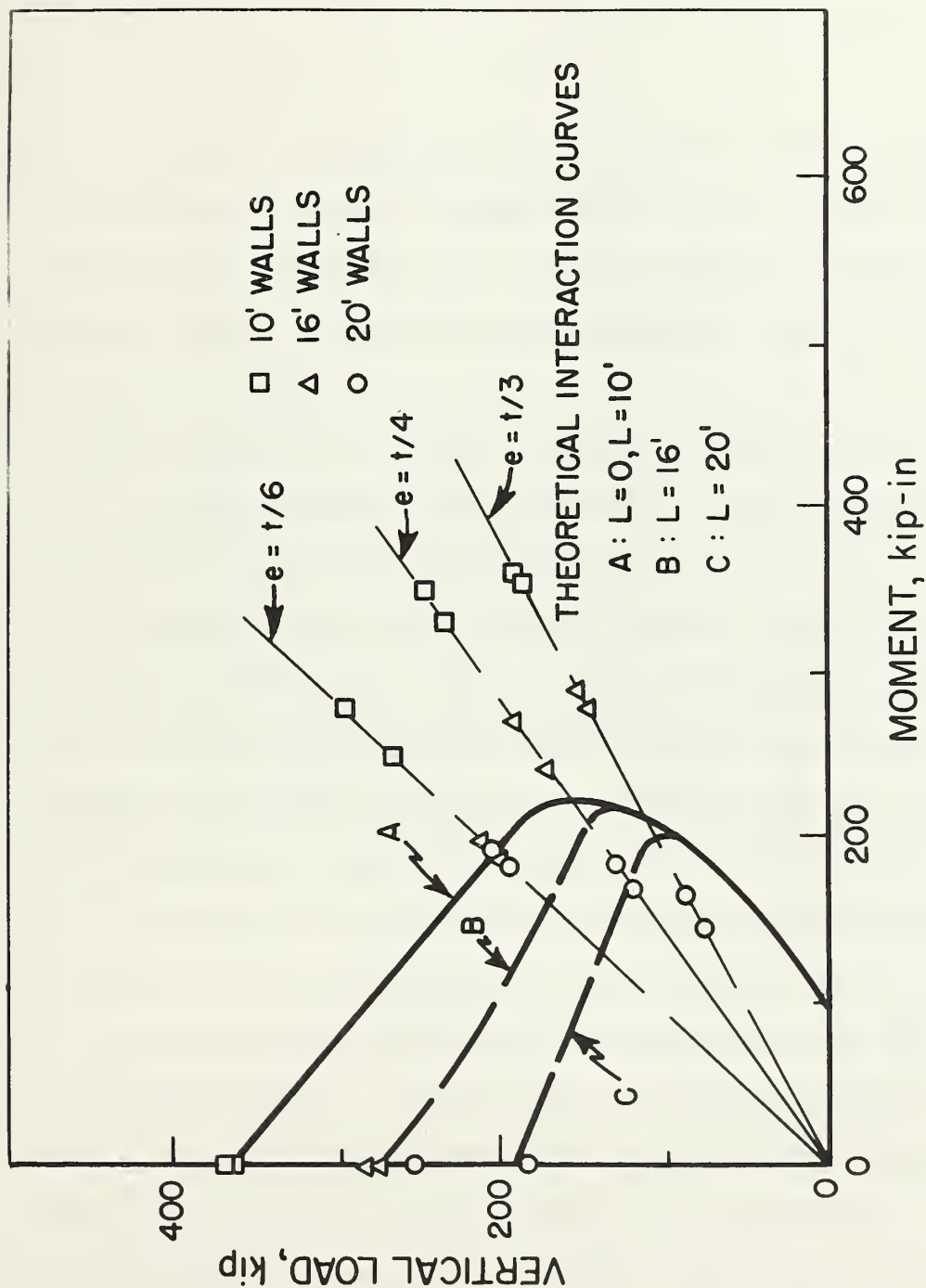ECCENTRICALLY LOADED REINFORCED WALLS

Fig. 6.8

ASSUMED CONDITIONS OF BASE FIXITY

Fig. 6.9

These assumed end conditions are conservative with
respect to the 16- and 20-ft walls.

(2) Slenderness effects: Figure 6.10 shows the test
esults of all the reinforced walls. Applied end moments
(Pe) are plotted against vertical load. It is evident
that the strength of the 16-ft and 20-ft walls was con-
siderably reduced by slenderness effects.

The solid curve (Curve A) in figure 6.10 is the short-wall
interaction curve for the section capacity of these walls,
developed on the basis of the average axial strength of
he 6-in prisms which was discussed in section 6.2. As
noted previously, this curve is very conservative with
respect to moment capacity. From this curve, interaction
curves for slender walls can be developed by reducing the
moment at each level of P by the moment magnifier equation.
Such reduced interaction curves were developed, using a C_m
value of 0.5, a k value of 0.8, and EI value of $E_i I_n/2.5$.

For the 10-ft high walls no slenderness effects are
predicted by the moment magnifier equation. Thus the
solid curve for section capacity is also the interaction
curve for the 10-ft walls. Curve B is the reduced inter-
action curve for the 16-ft walls. Comparison of this
curve with the test results of the 16-ft walls shows that

70

COMPARISON OF TEST RESULTS ON 6-IN REINFORCED
WALLS WITH THEORETICAL INTERACTION CURVES BASED
ON AXIAL PRISM STRENGTH

Fig. 6.10

the axial load, which is the critical load for stability-induced compression failures, was accurately predicted. Capacities under eccentric vertical loads are conservatively predicted.

Curve C (figure 6.10) is the computed interaction curve for the 20-ft walls. This curve closely predicts the axial strength of one of the 20-ft walls. The other wall developed significantly higher strength. This is probably attributable to the fact that this wall had a longer than average curing period. (This wall was tested at an age of 12-18 days, compared with the 7-13 day age of the lower strength wall.) The two 20-ft walls tested at t/6 eccentricity both developed strength considerably in excess of the predicted strength and developed strengths similar to that of the 16-ft walls. These walls also had a longer than average curing period (19-21 days). At the t/4 eccentricity the predicted strength is close to the observed strength. At the t/3 eccentricity wall strength is overestimated by the theory. At that eccentricity, in accordance with the failure description in table 5.2, the 20-ft walls developed a stability failure, where very large increments of deflection were associated with relatively minor increase in axial load. These two walls represent an extreme condition (h/t = 41, e/t =1/3) which is outside the range presently considered in the

design of slender masonry walls. At this extreme condition, wall stiffness EI is considerably reduced by section cracking. The expression $E_i I_n/2.5$ is an average stiffness reduction and does not consider the variable of progressive section cracking which is a function of P/P_o. When this expression was developed it was recognized that it is valid over a range of values of P/P_o, sufficient to cover all practical design cases. The extreme case of failure at a very low value of P/P_o is outside the range of the expression.

It may be concluded that except for the extreme case of 20-ft walls loaded at t/3 eccentricity the theoretical interaction curves are conservative.

It has been noted in section 6.2 that the interaction curve based on axial compressive prism strength is very conservative and that flexural compressive strength increases with increasing strain gradients. The dashed curve shown in figure 6.4 was developed on the basis of the flexural strength at the eccentricity of t/3 and is probably accurate or conservative for eccentricities greater than t/3. Reduced interaction curves, developed from this curve should therefore accurately predict the test results for values of P below the failure load for short walls at the t/3 eccentricity.

73

Figure 6.11 shows reduced theoretical interaction curves developed from this section capacity curve (curve A), together with the test results. Note that there is excellent correlation between Curve B, the theoretical interaction curve for 16-ft walls, and the test results. The solid portion of curve B, as well as the point at axial load are computed by theory. The lighter dashed portion is a straight-line interpolation between the computed axial capacity and the range covered by the solid curve, which is computed. Curve C, which was computed for the 20-ft walls shows good correlation with wall tests at the t/4 eccentricity and with one wall test at axial load. The other walls tested at axial load and the walls tested at t/6 eccentricity were stronger and the walls at the t/3 eccentricity failed at a lower than the predicted load, as previously discussed. On the whole, the trend of the test results, as well as actual failure loads are in good agreement with the theoretical predictions.
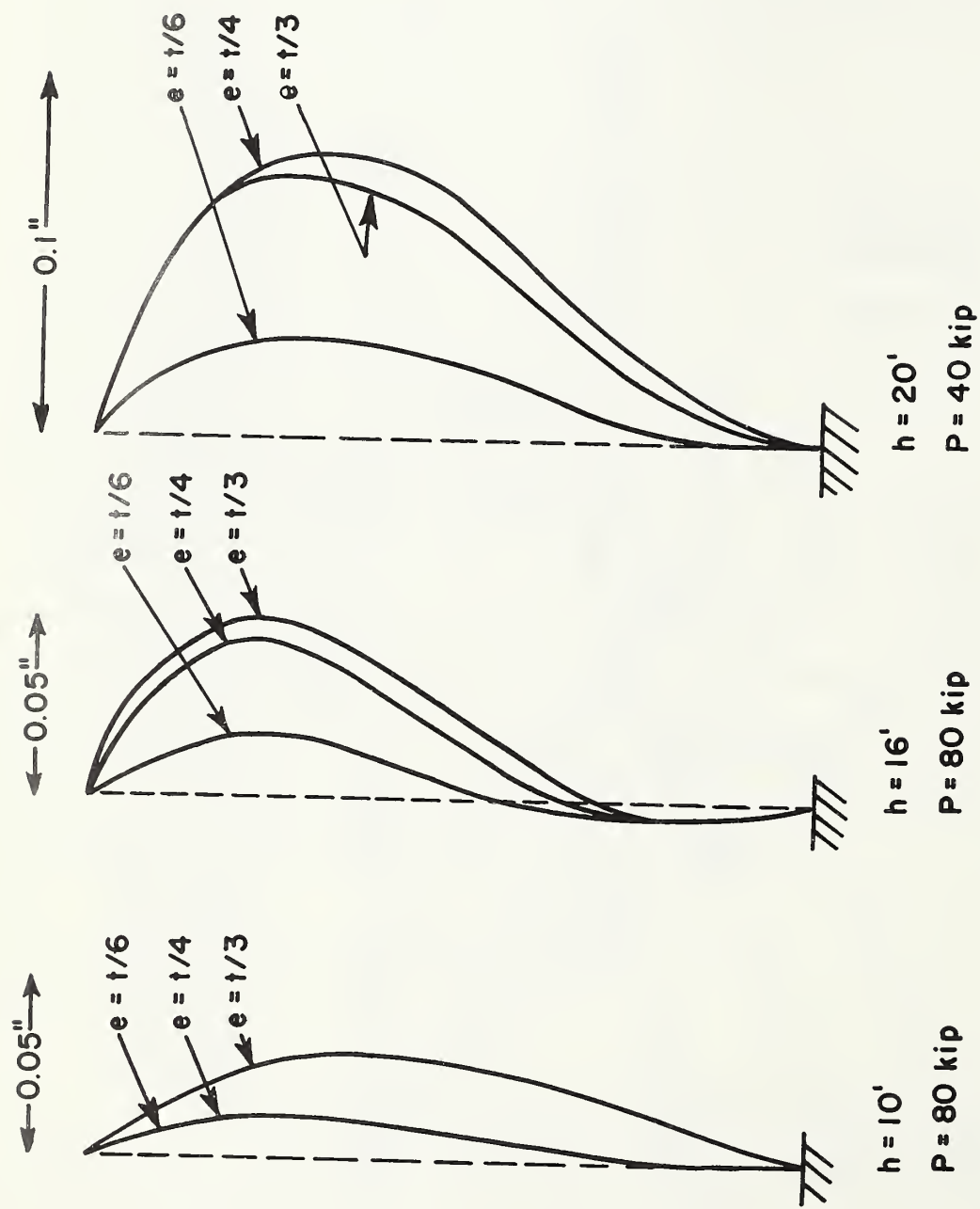
6.3.3 8-in Unreinforced Walls

(1) End fixity: Figure 6.12 shows measured deflection curves for the 8-in walls. Again it appears that the 10-ft walls developed only minor end restraint, while the 16-ft and 20-ft walls developed partial end fixity.

COMPARISON OF TEST RESULTS ON 6-IN REINFORCED
WALLS WITH THEORETICAL INTERACTION CURVES BASED.
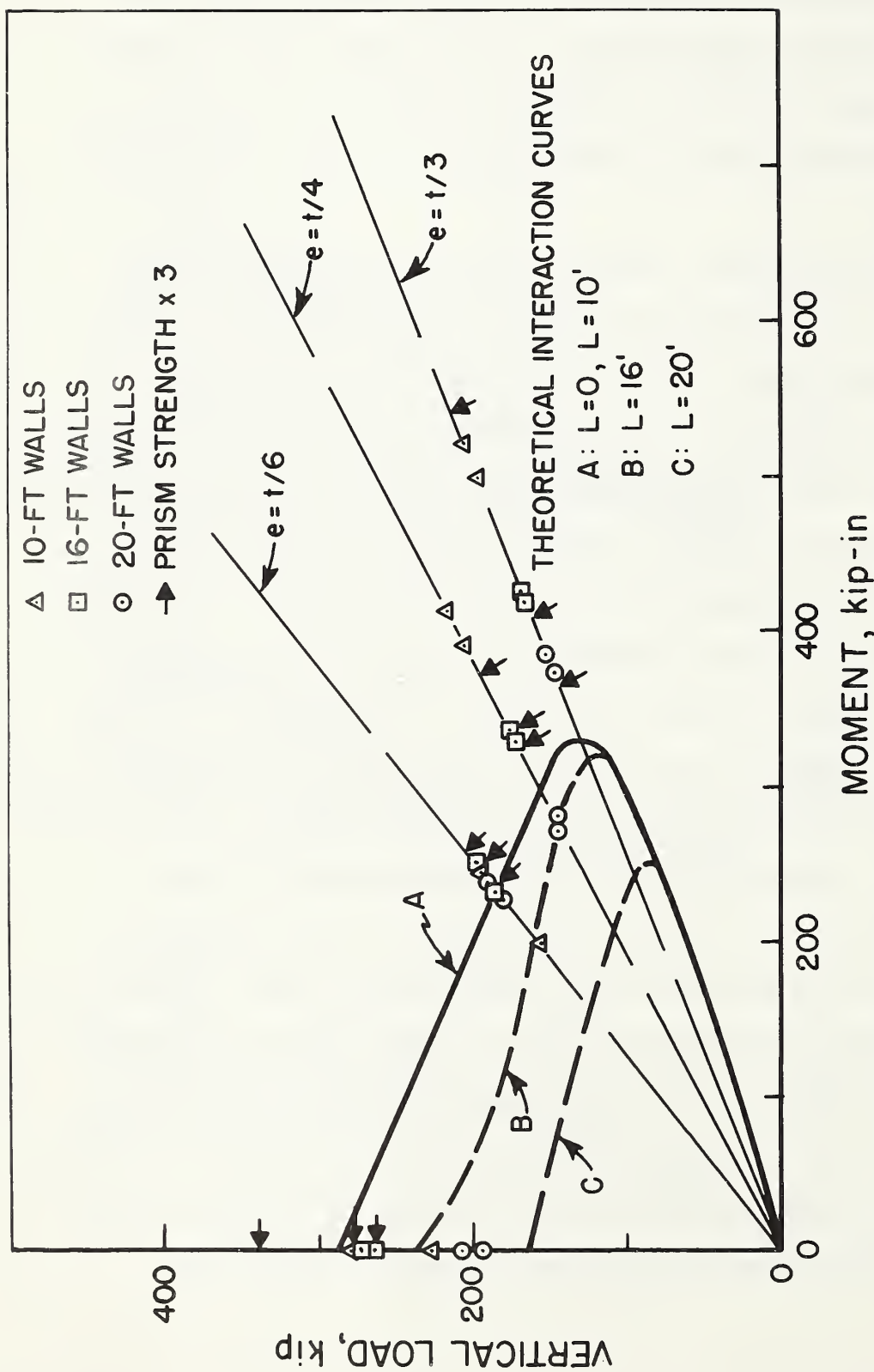ON FLEXURAL COMPRESSIVE STRENGTH

Fig.6.11

TYPICAL DEFLECTION CURVES FOR ECCENTRICALLY
LOADED UNREINFORCED WALLS

Fig. 6.12

The "negative" deflections measured in the 16-ft walls were probably caused by deformation of the aluminum pipes on which the LVDT's were mounted. In all other tests larger diameter pipe was used. Again it is assumed that base-fixity conditions were in accordance with figure 6.9.

(2) Slenderness effects: Test results of the 8-in wall panels are plotted in figure 6.13. Under axial load the two 20-ft walls and the two 16-ft walls failed at different load levels, and the average failure load of the 16-ft walls was considerably higher than that of the 20-ft walls. The 10-ft walls, however, showed a considerable discrepancy in failure load. One of these walls developed a failure load close to that of the 16-ft walls, and the other failed at a lower load. Two of the prisms failed at loads similar to the failure loads of the 16-ft walls and one prism developed greater strength than all other specimens. There appears to be a polarization of test results of the 16- and the 20-ft walls. The strength of the 10-ft walls and the prism strengths are such that no statistically significant effect of wall height on strength can be derived for walls up to the height of 16 ft.

At the t/6 eccentricity all the wall and prism tests except for one 10-ft wall test are concentrated between the

COMPARISON OF TEST RESULTS ON 8-IN UNREINFORCED
WALLS WITH THEORETICAL INTERACTION CURVES BASED
ON AXIAL PRISM STRENGTH

Fig. 6.13

failure loads of 280 to 305 kip. There appears to be no noticeable correlation between wall height and strength within the range of wall heights tested.
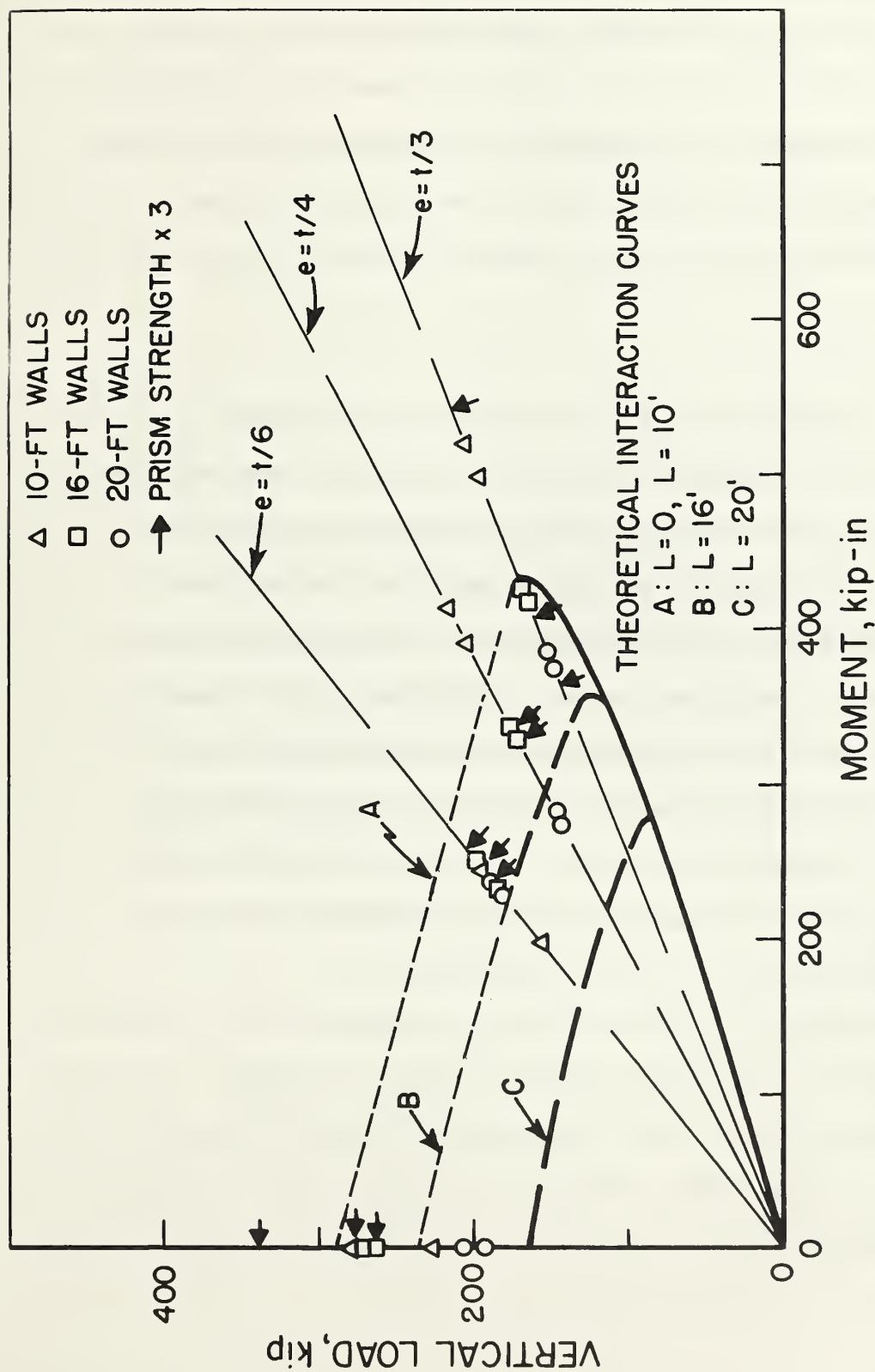
At the t/4 and t/3 eccentricities there is a definite polarization in accordance with wall heights. However, this observation is not supported by the prism strengths. At the t/4 eccentricity prism tests have an average similar to the average of all wall tests, and at the t/3 eccentricity there is a considerable variation in prism strength with a scatter over the entire range of wall strengths. Since at the maximum eccentricity any test will be close to the failure envelope of the section capacity, test results may be very sensitive to the precision of the positioning of applied loads. The possibility therefore, can not be ruled out that the polarization of these test results may be coincidental and that the spread of the results may represent normal strength variations due to material strength, workmanship and precision of load application.

The solid curve in figure 6.13 (Curve A) is the short-wall interaction curve developed on the basis of the average axial strength of the 8-in prisms. This curve was discussed in section 6.2 and it was concluded that, in general, this curve is conservative with respect to eccentric loads. Curves B and C are reduced interaction curves for the 16-ft

and 20-ft walls, respectively. These curves were developed
from Curve A by the moment magnifier method, using the
stiffness reduction derived for unreinforced masonry:
$EI = E_i I_n/3.5$. In accordance with the assumed end con-
ditions, a C_m factor of 0.5 was used, together with a k
factor of 0.8. Note that, in all cases, these reduced
interaction curves are conservative.

Figure 6.14 shows reduced interaction curves which were
developed from a short-wall interaction curve that is
based on the average prism strength at the t/3 eccentricity
(f'_m = 2,320 psi). As previously noted, this curve is
probably accurate or slightly conservative for eccentricities
greater than t/3. These reduced interaction curves should
be less conservative than the curves shown in figure 6.13
and should predict the ultimate strength of the walls more
closely. In figure 6.14, Curve A is the short-wall inter-
action curve, Curve B is for 16-ft walls and Curve C is for
20-ft walls. The solid portions of these curves were
computed by theory. The lighter dashed lines are straight-line
interpolations between the end point of the computed curves
and the computed axial loads. The reduced curves, thus
computed, are slightly conservative. This may be because
of the fact that at the t/3 eccentricity 10-ft wall strength
exceeded the average prism strength. At the t/3 and t/4
eccentricities, the order of magnitude of observed slenderness

80

COMPARISON OF TEST RESULTS ON 8-IN UNREINFORCED WALLS
WITH THEORETICAL INTERACTION CURVES BASED ON FLEXURAL
COMPRESSIVE STRENGTH

Fig. 6.14

effects is in good agreement with the magnitude of com-
puted slenderness effects. This is also true with respect
to the 16-ft and 20-ft walls under axial loads. In all
these cases the reduced interaction curves are conservative.
At the t/6 eccentricity the wall tests show no correlation
between length and ultimate load, however, the reduced
curves are conservative with respect to the 16-ft and 20-ft
walls.

It may be concluded from the discussion of figures 6.13
and 6.14, that strength of slender walls was conservatively
predicted by the moment magnifier method, assuming that
the flexural compressive strength of the masonry equals
the average axial prism strength, and that the order of
magnitude of slenderness effect, as well as the strength
of slender walls were approximately predicted by the
moment magnifier method, when the flexural compressive
strength of masonry at load eccentricities greater than
t/3 was assumed to equal the average flexural strength
of prisms, loaded at a t/3 eccentricity.

7. DISCUSSION OF PRESENT DESIGN PROCEDURES

The latest recommended design procedures for eccentrically loaded slender concrete masonry walls are presented in the 1968 NCMA standard [2]. This standard requires that members subject to eccentric loads be proportioned such that:

$$\frac{f_a}{F_a} + \frac{f_m}{F_m} \leq 1 \qquad (5)$$

where:

f_a = Computed axial compressive stress equal to the total vertical load divided by the net area,

F_a = Compressive stress permitted by the standard for axial loading,

f_m = Computed flexural stress,

F_m = Flexural compressive stress permitted by the standard.

The allowable compressive stress under axial loading is reduced for slenderness effects, using a reduction factor of $[\ 1 - (\frac{h}{40t})^3\ ]$. The allowable short-wall axial stress is $0.2f'_m$ for unreinforced masonry and $0.225f'_m$ for reinforced masonry. Allowable flexural compressive stresses are $0.3f'_m$ and $0.33f'_m$ for unreinforced and reinforced
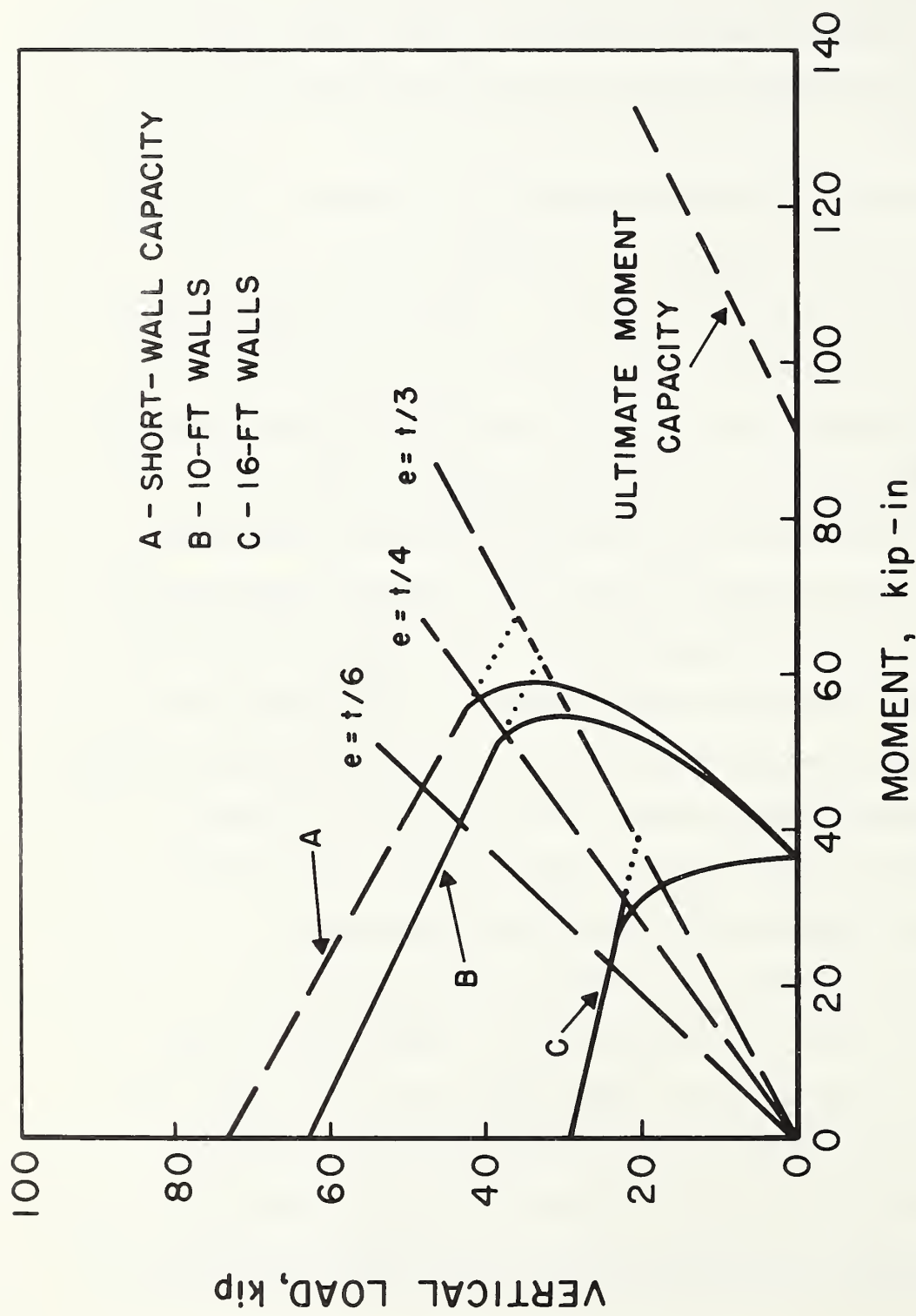
masonry, respectively. The standard does not permit
tensile stresses in unreinforced masonry walls built with
hollow units, thus limiting load eccentricity to the edge
of the kern. For solid unreinforced masonry and for rein-
forced masonry cracked sections are permitted. It is also
stated in the standard, that up to a load eccentricity of
t/3, reinforced walls may be designed on the basis of an
uncracked section.

These design recommendations consider wall slenderness,
however the h/t ratio does not take the mass-distribution
within the cross section into account, and therefore does
not differentiate between solid and hollow sections.
Other variables associated with slenderness effects and
not considered in these design equations are end fixity
effects (effective length),[2] the effect of the manner in
which the member is loaded (the shape of the moment diagram
and the resultant deflection curve), and the relationship
between the strength and the modulus of elasticity of the
masonry.

---

[2] Some general consideration is given in NCMA Standard to
cantilever members and members subject to sidesway.

84

A short-wall interaction curve can be developed using
the recommended interaction equation, eq(5), the allowable
axial and flexural stresses, and the other requirements
contained in the NCMA standard as mentioned previously.

Figure 7.1 shows interaction curves of allowable vertical
loads and moments, computed for the 6-in reinforced
masonry walls by the NCMA standard. Masonry strength f'_m
was taken as the average axial compressive strength of the
6-in three-block prisms tested in the investigation reported
herein. The dashed curve (A) was computed without any
slenderness reduction and represents short-wall capacity.
The solid curves labeled B and C were computed for the 10-ft
and the 16-ft walls, respectively. The dashed radial lines
represent the load eccentricities used in the tests. The
intersection points of these radial lines with the interaction
curves represent the allowable vertical loads at these
eccentricities. Note that the upper, linear part of the
interaction curves, which represents capacities
of uncracked sections, is extended in each case by a
dotted line to the t/3 eccentricity. These dotted lines
correspond to the provision that walls may be designed for
uncracked sections up to the t/3 eccentricity. Curve C,
which corresponds to an h/t ratio of 34, is actually an
extrapolation of the NCMA standard which limits the h/t

A - SHORT-WALL CAPACITY
B - 10-FT WALLS
C - 16-FT WALLS

ULTIMATE MOMENT CAPACITY

e = t/6
e = t/4
e = t/3

MOMENT, kip-in

VERTICAL LOAD, kip

ALLOWABLE LOADS ON 6-IN REINFORCED WALLS
(NCMA, 1968)

FIG 7.1

ratio for load bearing reinforced walls to 30. The NCMA
equation could not be used to develop an interaction
curve for the 20-ft walls, since the equation for slender-
ness reduction goes to 0 at an h/t ratio of 40.

Computed allowable loads for the 6-in reinforced walls and
average ultimate strengths of the test specimens are com-
pared in table 7.1. Margins of safety were computed in
two ways: The ratio of average ultimate loads to allowable
loads was computed for specific load eccentricities, and
the ratio of ultimate moments to allowable moments was
computed for specific levels of vertical loads.

The first case pertaining to a constant load eccentricity
involves a radial "scaling down" of the ultimate inter-
action diagram, indicates the margins of safety against an
increase in vertical loads, acting at the same eccentri-
city. In a building, this would correspond approximately
to an increase in occupancy load above the design load
level. The margins of safety for this case are given in
table 7.1. For the 10-ft walls they vary from 5.7 to 6.5.
For the 16-ft walls the margins of the safety vary from
7.5 to 9.9. It appears that these margins of safety are
quite high for short walls, and, for the end conditions
applied in this investigation, they increase for increasing
wall slenderness.

TABLE 7.1 Comparison of Allowable Loads with
Average Ultimate Load Capacities of 6-in
Reinforced Walls

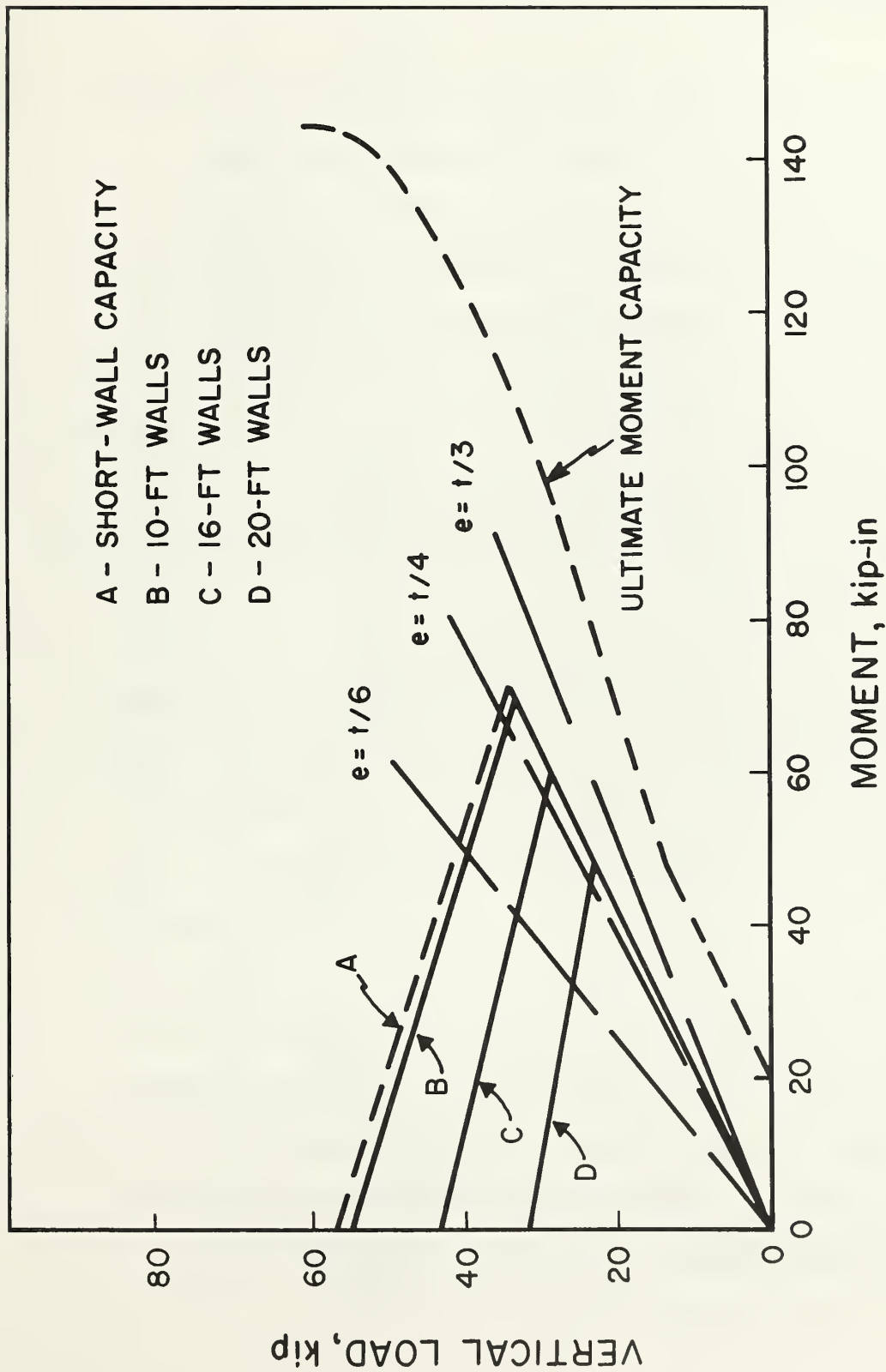| Wall Length ft	e/t	Case 1			Case 2		
		Allowable Vertical Load kip	Average Ultimate Vertical Load Capacity kip	Ultimate Load / Allowable Load	Allowable Moment kip-in	Computed Ultimate Moment At Allowable Vertical Load kip-in	Ultimate Moment / Allowable Moment
10	0	63	365	5.8	0	210	∞
	1/6	43	280	6.5	40	175	4.4
	1/4	38	242	6.4	52	165	3.2
	1/3	29(33)a/	188	6.5(5.7)	54(62)	148	2.7(2.4)
16	0	28	278	9.9	0	147	∞
	1/6	24	207	8.6	23	140	6.1
	1/4	21(22)	181	8.6	30	135	4.5
	1/3	18(20)	150	8.3(7.5)	34(38)	129	3.8(3.4)

a/ Numbers in paranthesis are computed on the basis of an uncracked section.

The second case, which pertains to a constant vertical load, while increasing the moment acting on the wall, corresponds to a horizontal scaling down of the ultimate interaction diagram. In a building this would correspond to an increase in horizontal live loads (wind loads) without a corresponding increase in vertical live loads. The margins of safety for this second case are also presented in table 7.1. It is important to note, that within the limit of vertical loads presently permitted in design, ultimate moments increase with vertical loads. At the maximum permitted vertical load, at which no moment is permitted in the NCMA standard, the walls can actually support a greater ultimate moment than at any lower vertical load. For eccentric loads the margins of safety vary from 2.4 to 4.4 for the 10-ft walls and from 3.4 to 6.1 for the 16-ft walls. It is apparent that the safety margins decrease with increasing load eccentricity. It can also be observed that the safety margins are greater for the more slender walls.

The ultimate moment capacity is shown by a dashed line in figure 7.1. It appears that much of the margin of safety is due to the high ultimate moment at no vertical load which is attributable to the reinforcement. Since the specimens in this investigation had about twice the minimum required reinforcement, it may be concluded that

89

for walls with minimum reinforcement, margins of safety
may have been smaller. When margins of safety for Case 1
are compared with those given for Case 2, it is apparent
that for eccentricities greater than t/6, and particularly
for large eccentricities, the margin of safety against an increase in horizontal live loads is substantially smaller
than that provided against an increase in vertical live
loads. Thus, it may be concluded that reinforced walls,
designed in accordance with present practice have a greater
and more uniform margin of safety with respect to vertical
live loads than the margin provided with respect to
horizontal live loads.

Figure 7.2 shows interaction diagrams for allowable vertical loads and moments, computed by the NCMA standard for
the 8-in unreinforced masonry walls. Curve A is the
short-wall interaction curve, and curves B, C, and D are
for the 10-ft, the 16-ft and the 20-ft walls respectively.
Note that the interaction curves are cut off at the kern
eccentricity, which is slightly larger than the t/4
eccentricity. Thus the t/3 eccentricity falls outside
the curves, since it is not permitted under this standard.
The dashed line to the right of the curves is the computed
short-wall ultimate moment capacity which was based on the
flexural compressive prism strength at the t/3 eccentricity.
Curves C and D are extrapolations of the NCMA standard, which

90

ALLOWABLE LOADS ON 8-IN UNREINFORCED WALLS
(NCMA, 1968)

FIG 7.2

limits the maximum h/t ratio to 20 for unreinforced load-bearing walls.

Computed allowable loads for the 8-in unreinforced walls are compared in table 7.2 with the average ultimate strengths achieved by the test specimens. Margins of safety against an increase in vertical loads applied at the same eccentricity (Case 1), vary from 4.4 to 6.4 for the 10-ft walls, from 5.8 to 6.2 for the 16-ft walls, and from 6.0 to 7.1 for the 20-ft walls. In general it appears, for the particular end and loading conditions used in this investigation, that these margins of safety are quite uniform and on the high side.

Safety margins against an increase in moments at the same vertical load (Case 2) are also given in table 7.2. As in the case of the 6-in reinforced walls, these margins of safety decrease with increasing eccentricity, dropping to 1.75 at the t/3 eccentricity. It is important to note, that for unreinforced walls built of solid units, which can be designed on the basis of a cracked section, these margins of safety may drop even lower and approach unity. Thus, while margins of safety against an increase of vertical loads are rather high, the margins against an increase in horizontal loads may be extremely small.

TABLE 7.2 Comparison of Allowable Loads With
Average Ultimate Load Capacities of
8-in Unreinforced Walls

Wall Length ft	e/t	Case 1			Case 2		
		Allowable Vertical Load kip	Average Ultimate Vertical Load Capacity kip	Ultimate Load / Allowable Load	Allowable Moment kip-in	Computed Ultimate Moment at Allowable Vertical Load kip-in	Ultimate Moment / Allowable Moment
10	0	57	252	4.4	0	144	∞
	1/6	39	177	4.5	50	122	2.4
	1/4	33	210	6.4	63	110	1.75
16	0	43	268	6.2	0	129	∞
	1/6	33	191	5.8	42	108	2.6
	1/4	30	174	5.8	57	100	1.75
20	0	32	202	6.3	0	105	∞
	1/6	26	184	7.1	33	88	2.7
	1/4	24	143	6.0	46	80	1.75

93

The allowable vertical loads and moments shown in figures 7.1 and 7.2 and listed in tables 7.1 and 7.2 were based on the average axial compressive strengths of the prisms as determined by tests. For the 6-in prisms, f'_m was 1890 psi and for the 8-in prisms, f'_m was 1700 psi. If f'_m values are not determined by tests, the NCMA standard permits f'_m values to be assumed on the basis of the unit strengths. For the 6-in and 8-in hollow concrete block used in this investigation which had strengths of 4080 psi and 4230 psi (net area), respectively, the assumed values of f'_m permitted are 2017 psi and 2047 psi. Based on this investigation, the assumed values of f'_m permitted in the NCMA standard are about 7% too high for the 6-in prisms and about 20% too high for the 8-in prisms. Accordingly, if these assumed values of f'_m were used in the comparisons given in tables 7.1 and 7.2, the margins of safety would be smaller than the values reported.

Three important conclusions may be drawn from this discussion:

(1) Present design criteria provide a large margin of safety with respect to vertical loads. This margin of safety is necessary, since present design procedures do not account for all the variables that affect wall capacity.

The most important variables not accounted for are end fixity, the shape of the moment diagram that acts on the wall, cross-sectional characteristics, and the modulus of elasticity of the masonry. In the past, it may not have been justified to account for all these variables, since design standards also contained rather restrictive requirements relating to allowable stresses, lateral support and minimum thicknesses of masonry bearing walls. However, with the increasing use of masonry load-bearing walls in multi-story construction, it is no longer justified to disregard these variables and compensate for the resulting discrepancies by excessive margins of safety.

The close prediction of experimental results in this investigation by the moment magnifier method indicates that the introduction of a rational design method which considers additional variables is practically feasible.

(2) The margin of safety provided by present design practice against an increase in moment, without a corresponding increase in vertical load, is in some cases extremely small. On the other hand, at maximum allowable vertical load, no moment is permitted, while it appears that at that load the wall actually develops the highest ultimate moment capacity. It appears that the philosophy

of "radial scaling" which is presently applied to develop allowable wall capacities on the basis of ultimate capacities leads to excessive margins of safety in some cases, while in other cases the margins of safety are extremely slim.

The philosophy behind the scaling down of ultimate loads in order to arrive at reasonable design loads should be reexamined, and all possible load combinations that may act on masonry walls during the life of a building should be taken into account.

(3)   Based on the prism strengths obtained in this investigation, the assumed values of axial compressive strength f'_m permitted for hollow concrete units in present design criteria are too high and should be reexamined.

8.   CONCLUSIONS AND RECOMMENDATIONS

8.1   Conclusions Related to Test Results

The following conclusions can be derived from the inter-
pretation of the test results:

(1)   Theoretical interaction curves for the capacity of
short concrete masonry walls, computed on the basis of
compressive strength developed by masonry prisms under
axial loading, closely predict axial compressive load
capacity and conservatively predict moment capacity.

(2)   Flexural compressive strength of masonry increases
with increasing strain gradients (increasing load eccentri-
city).

(3)   Slender concrete masonry wall capacity can be con-
servatively predicted by the moment magnifier method, when
short-wall capacity is based on compressive strength of
axially loaded prisms.

(4)   The capacity of short and slender concrete masonry
walls can be predicted with reasonable accuracy when the
increase in flexural compressive strength with increasing
strain gradients is taken into account.

97

8.2 Conclusions Related to Present Design Practice

The following conclusions can be derived from the review of present design practice:

(1) Present design criteria [2] provides a large margin of safety with respect to vertical loads on load bearing concrete masonry walls but the margin of safety provided against an increase in moment, without an increase in vertical loads, is not uniform and in some cases extremely small.

(2) Introduction of a rational design procedure such as the moment magnifier method which includes additional design variables not presently considered is feasible and appears desirable in the interest of safety and economy.

(3) Assumed values of masonry compressive strength permitted in present design criteria are too high for hollow unit construction and should be reexamined.

8.3 Additional Research Required

Based on this program and a review of other pertinent investigations, the following additional research has been identified:

(1) Investigation of stress-strain properties and short-wall section capacity. The objective of this investigation would be to predict short-wall section capacity for unreinforced and reinforced concrete masonry walls on the basis of small specimen tests. It should include a thorough investigation of the relationship of compressive strength to varying strain gradients and to the modulus of elasticity.

(2) Investigation of slenderness effects. The objective of this investigation would be to study the slenderness effects on concrete masonry wall strength. It should include an investigation of various conditions of end fixity and various loading conditions (eccentric vertical loads, combined axial vertical and transverse loads and combinations of these two modes of loading).

9. ACKNOWLEDGEMENT

10. REFERENCES

[1] National Building Code of Canada, Ottawa, Canada, (1965).

[2] National Concrete Masonry Association, Specification for the Design and Construction of Load-Bearing Concrete Masonry, Arlington, Virginia, (1968).

[3] Sampling and Testing Concrete Masonry Units, ASTM C140-65T (1965).

[4] Mortar for Unit Masonry, ASTM C270-68 (1968).

[5] Mortar and Grout for Reinforced Masonry, ASTM C476-63 (1963).

[6] W. L. Dickey, Reinforced Brick Masonry, Modern Masonry Conference, Washington, D.C., September 19-20, 1956; Building Research Institute, National Academy of Sciences-National Research Council, Publication 466 (1956).

[7] Deformed Billet-Steel Bars for Concrete Reinforcement, ASTM A615-68 (1968).

[8]   F. Y. Yokel, R. G. Mathey and R. D. Dikkers, Effect
      of Vertical Compressive Loads on the Transverse
      Strength of Masonry Walls, National Bureau of
      Standards Report No. 10139, December 1969.

[9]   J. G. MacGregor, J. E. Breen and E. O. Pfrang,
      The Design of Slender Concrete Columns, Presented
      at the 65th Annual Convention, American Concrete
      Institute, April 1969.

[10] Structural Clay Products Institute, Recommended
      Practice for Engineered Brick Masonry, McLean,
      Virginia (1969).

Joint Thickness Study

Scope

Twenty-three three-block high prisms, capped with high
strength plaster, were tested under axial load. The test
variables and the number of specimens tested are shown
in the following table.

Age	Joint Thickness			
	3/8-in	1/2-in	5/8-in	3/4-in
7-days	3	3	3	3
28-days	3	3	3	2

Materials

The block were 8 x 8 x 16-in two-core hollow units. Com-
pressive strength of the masonry units was 1220 psi,
based on gross area. Mortar strength was 970 psi at 7
days and 1630 psi at 28 days.

Results

Failure mode was generally vertical splitting. First
cracks developed at approximately 90% of ultimate failure
load. Test results are shown in figure A.1.

Conclusions

No statistically significant trend can be observed for
the prism compressive strength to decrease with increasing
joint thickness. However, for joints thicker than 1/2-in,
there is a significant increase in the strength variation
between individual test results.

RELATIONSHIP BETWEEN APPLIED LOAD AND MORTAR
JOINT THICKNESS FOR 3-BLOCK HIGH PRISMS

FIG A.I